Bank of England

# Measuring the stability of the banking system: capital and liquidity at risk with solvency-liquidity interactions

**Staff Working Paper No. 1,140**
August 2025

**Giovanni Covi and Tihana Škrinjarić**



Bank of England

Staff Working Paper No. 1,140

# Measuring the stability of the banking system: capital and liquidity at risk with solvency-liquidity interactions

Giovanni Covi[1] and Tihana Škrinjarić[2]

## Abstract

This study develops a stochastic balance sheet based microstructural banking model to quantify the dynamic interplay between solvency and liquidity risks – two traditionally distinct dimensions in stress testing. By incorporating endogenous bank reactions, feedback loops, and amplification mechanisms, the model captures how management responses to shocks can escalate financial distress, potentially leading to insolvency and illiquidity. We apply the model to granular loan and security exposure data from UK banks over 2015–24, estimating capital and liquidity at risk and deriving a systemic default probability indicator. Results indicate an average one-year bank default probability of 0.7%, consistent with market-implied estimates but diverging during stress episodes. Amplification effects, driven by balance sheet constraints and behavioural responses, account for approximately one third of default risk on average. Counterfactual analyses further evaluate the effectiveness of capital requirements and identify optimal capital levels under hypothetical stress scenarios.

**Key words:** Banking stability, solvency-liquidity interactions, financial contagion, macroprudential stress test.

**JEL classification:** D85, G21, G32, L14.

---

(1) Bank of England. Email: giovanni.covi@bankofengland.co.uk
(2) Bank of England. Email: tihana.skrinjaric@bankofengland.co.uk



We are grateful to Kirstine McMillan, Joseph Clouting, Joanna McLafferty, Joseph Smart, Ashley Young, Joshua Lillis, Kishore Kamath, Rhiannon Sowerbutts, Grellan McGrath, Geoff Coppins, Matthew Waldron, George Speight, Rebecca Maule, and all the participants at FS seminar series for comments and stimulating discussions.

The Bank's working paper series can be found at www.bankofengland.co.uk/working-paper/staff-working-papers

Bank of England, Threadneedle Street, London, EC2R 8AH
Email: enquiries@bankofengland.co.uk


ISSN 1749-9135 (on-line)

## 1. Introduction

On March 8 2023, Silicon Valley Bank (SVB) experienced the most classic text-book example of a bank run which resulted in total deposit withdrawals of $42 billion in one single day, almost 25% of its funding structure. To offset this liquidity needs and repay its depositor base, SVB sold $21 billion of US Treasury bills (T-bills) and thus realized $1.8 billion of marked-to-market (MtM) losses which further triggered a loss of confidence in the bank. This caused a rating downgrade which brought an additional $100 billion of deposit withdrawals scheduled for the day after. SVB could not pay these obligations and was declared insolvent on March 10 2023 (FED, 2023). SVB didn't manage the interest rate risk associated with its securities holdings, heavily concentrated in long-term US Treasury bonds. The bank had a concentrated business model - not only on the asset side - but also on the liability side with its funding structure being strongly reliant on uninsured deposits from venture capital firms.

SVB's collapse was not caused by any single risk factor, but rather by the interaction of several. While funding concentration or interest rate exposure alone would not have triggered its default—especially since its assets were mainly liquid T-bonds—the combination of solvency and liquidity risks rapidly escalated the situation. This dynamic turned a stable bank into an insolvent one within days during the 2023 US Regional Banking Crisis, which also saw the failures of Signature Bank and First Republic Bank. The resulting market uncertainty blurred distinctions between banks, leading to widespread "news" and "market contagion" that affected even major US and global banks. In the end, in March 2023, Credit Suisse's default highlighted that even a Global Systemically Important Bank (GSIB) could fail despite central bank support. Although still solvent, fears over its profitability led to significant client withdrawals—around 10% of its assets. To prevent broader market disruption, UBS acquired Credit Suisse under favourable terms on March 19. This event, along with others, demonstrated that funding shocks and fire-sale dynamics can affect even high-quality assets like government bonds. These shocks now unfold faster than before, acting as both triggers and amplifiers of solvency crises.

Against this background, this work aims to develop a framework for assessing, monitoring, and testing banking stability as a joint assessment of both solvency and liquidity risks and their interactions. We rely on a stochastic microstructural accounting-based network methodology to model granularly the complex set of banks' relationships on an exposure level maintaining a stock-flow consistent approach at a bank balance sheet level on the asset side as well as on the liability side (Montagna et al., 2020; Sydow et al., 2024; Covi and Huser, 2024). Our framework extends the existing approach by jointly modelling shocks on the asset and liability

side simultaneously, which captures solvency and liquidity risks and their correlations. Moreover, we include multiple financial contagion channels after the initial shock. Thus, we model the interaction between solvency and liquidity risk in a correlated manner. Also, we calibrate banks' cost of funding as a function of their solvency position and the level of market distress endogenously in the model.

Given this detailed representation of the banking system and accounting relationships which are fully endogenized, we can use this framework to test counterfactual hypotheses and scenarios and assess in comparative terms the marginal impact of those changes as deviations to baseline estimates. To achieve this, we compute a distribution of outcome variables which capture aggregate vulnerabilities at a system level, respectively a profit and loss distribution, funding outflow distribution, as well as regulatory ratios distribution which combine information from the two previous distributions and banks' balance sheet characteristics. Accordingly, we derive three main risk metrics, respectively Conditional Capital at Risk (CCaR) representing the Value at Risk of banks' profit and loss distribution, Conditional Liquidity at Risk (CLaR) representing the Value at Risk of banks' funding outflow distribution, and third the 1-Year average bank default probability for the banking system, our key outcome variable tracking financial (in)stability in banking.

We construct the most comprehensive supervisory granular banking exposure dataset covering both the asset and liability sides of the seven major UK banks. We then calibrate and test the methodology on a quarterly frequency over a 10-year period (2015q1-2024q1) which is representative of relevant stress episodes, regulatory reforms as well as policy interventions.

We obtain a rich set of results. We quantify that the 1-year average bank default probability for the UK banking system stands at 0.3% as of 2024q1, down from the peak of 1.2% reached during the pandemic period (2020q1), and below the historical 10-year average of 0.7% (2015-2024). This estimate seems to be aligned with equity-based market estimates during normal times, although some differences arise during stress periods like the Covid-19 pandemic, highlighting an overshooting tendency of market estimates relative to our microstructural accounting-based estimates.

Second, we find that banks most commonly default due to simultaneous breach of both capital and leverage ratios, with some heterogenous effects across time. The liquidity constraint seems to be the least binding in this period of analysis, given the high level of banks' cash reserves.

Third, we quantify and provide evidence on the effectiveness of the dividend restriction crisis tool implemented in early 2020 in curbing the average bank default probability, showcasing

the key role played in offsetting potential additional feedback and amplification mechanisms. This result holds when we test this policy on a GFC-type stress scenario.

Fourth, from a liquidity angle, we find that Conditional Liquidity at Risk (CLaR99) tracking the size of funding shocks at the 99th percentile decreased from 10% to 6% (share of total withdrawable deposits) between 2015 and 2024, roughly 20-30% of the LCR 30-days liquidity outflows assumption. Nonetheless, we find that CLaR99 estimates conditional to an adverse stress scenario (GFC-type event) may increase up to the severity of liquidity outflows assumed in the LCR (£850 billion), thereby corroborating its calibration under stress conditions.

From a solvency angle, we find that the most important channel of potential loss propagation between 2015 and 2024 is direct credit and market risk losses which average around £87 billion [of CCaR99], representing roughly 69% of total CCaR99 variation. Next, we find that the fire-sale channel is the second most relevant channel at play, with an average impact at 99th percentile of £23 billion of losses (18% of total CCarR99 variation). The impact varies materially over time (and across banks) between 15% and 28% depending (among other factors) on banks' security portfolio composition.

The reminder of the paper is structured as follows. Section 2 provides a summary of the main contributions of the paper in relation to the existing literature. Section 3 covers the methodological framework. Section 4 covers the data section and model calibration. Section 5 presents and discuss the model outputs and findings. Section 6 provides a macroprudential impact assessment of policy interventions gauging their effectiveness. The last section concludes.

## 2. Literature Review

Our approach builds on the model by Elsinger et al. (2006), as it allows us to capture the network of mutual credit exposures among banks which are influenced by shared macroeconomic conditions. This banking system-wide perspective reveals vulnerabilities that may be overlooked when supervisors focus only on individual institutions. As such, our work contributes in two key ways: first, by improving the methodology used to assess systemic risk; and second, by generating new insights that help evaluate the effectiveness of prudential regulation. Importantly, our results provide a risk assessment at the level of the entire banking system (macroprudential), rather than just individual banks (microprudential).

### *2.1 Methodological Contribution*

We follow this stream of literature (Montagna et al., 2020; Covi et al., 2022, 2024; and Sydow et al., 2024) and model banks' credit, market and liquidity risks as a function of banks' asset

and funding networks of exposures. On top of that we add feedback and amplification mechanisms as a function of banks' individual responses to shocks conditional to a set of balance sheet constraints. Our holistic approach contributes to the measurement and assessment of financial stability risks and to the calibration of prudential banking regulation via an integrated solvency-liquidity macroprudential stress test framework (Aikman et al., 2023)[1]. We start by modelling portfolio credit risk on an obligor-basis relying on the widely used Gaussian copula model described in Glasserman (2004; 2005) consistently with Covi et al. (2022; 2024) and Sydow et al. (2024). In this respect, this element allows us to model the dependence structure of obligor defaults and thus capture credit and traded risks stemming from correlated portfolio of loan and security exposures - the main source of systemic risk according to Elsinger et al. (2006). We then augment the simulation engine with a bank-specific net operating income component which is modelled as an inverse function of the severity of the realized loss in each simulation. This is consistent with findings from Bolt et al. (2012), and Albertazzi and Gambacorta (2009), and the approach derived in Covi and Huser (2024). This feature is often overlooked in most of the financial contagion literature, though it has important mitigating effects given net operating income may absorb shocks to banks' capital base via the retained earnings channel.

Next, we expand the simulation engine to encompass also funding shocks stemming from banks' correlated portfolios of deposits and repo activities. Hence, we model jointly and consistently shocks on the asset and liability sides of banks, thereby capturing solvency and liquidity risks and their potential correlation due to the overlapping set of counterparties. To the best of our knowledge, this is the first model that endogenize liquidity risk via a granular network of funding sources consistently with the network of obligors on the asset side.

In terms of feedback and amplification mechanisms, we combine multiple financial contagion channels and model the interaction between solvency and liquidity risks in a correlated manner, thereby making it mutually reinforcing, and so capture non-linear dynamics as discussed in the relevant literature (Cont et al., 2020; Hałaj, 2020; Aldasoro and Faia, 2016). Specifically, the methodology incorporates multiple channels—bank-runs, funding costs, fire-sales, and interbank contagion. A key novelty is the endogenous and empirical modelling of bank-runs and funding costs based on banks' characteristics and market distress. Bank-runs are triggered by breaches in capital and leverage buffers (Covi et al., 2019; 2021; Sydow et al. 2024),

[1] BCBS (2015) advises that integrated tests are desirable opposed to a stand-alone test, as the interaction between solvency and liquidity is often material.

extending beyond interbank withdrawals to all short-term funding from banks and financial corporates. After estimating funding outflows, we derive banks' total funding demand and the supply of secured and unsecured repo funding in the Sterling market, calculating the resulting additional funding costs. If unmet, these shocks may lead to fire-sales. This approach extends Cont et al. (2020) by incorporating system-wide contagion and endogenous funding dynamics at both the bank and system level. The methodological contribution is also related to the modelling and calibration of banks' cost of funding as a function of a bank's solvency position and the level of market distress. This is a major difference compared to the literature since the interest rate spread is endogenously derived (Dent et al., 2021; Babihuga and Spaltro, 2014; Korsgaard, 2021; Hasan et al., 2016; Arnould et al., 2022). Overall, in the literature there are clear evidence that, when controlling for bank-specific characteristics, a deteriorated solvency position negatively affects funding costs, with the relationship being non-linear. Although theory recognizes the interaction between the two risks (Rochet and Vives, 2004; Diamond and Rajan, 2005), integrating the two in stress testing has been lacking, both in empirical research (Cont et al., 2020), and in central bank implementation (Anderson et al., 2018). In this respect, we follow Hałaj (2018, 2020) who develops a system-wide ABM (agent-based model) model to capture liquidity and solvency risk interactions.

Next, we model fire-sale spillovers taking place via indirect price-mediated contagion as key feedback and amplification channel (Shleifer and Vishny, 2011; Greenwood et al., 2015; Caccioli et al. 2015, Cont and Schaanning, 2019; Duarte and Eisenbach, 2021; Caccioli et al. 2024; Sydow et al., 2024; Covi et al. 2024). In this respect, we rely on the existing literature and design a fire-sale mechanism whose deleveraging process is a function of both banks' leverage and liquidity needs (binding constraints) and affects the risk-weighted capital constraint. Thus, we construct a leverage targeting constraint which is bank-specific and adjusted to account for the bank-specific leverage volatility preference. We implement this feature as acknowledged by Caccioli et al. (2014), and Cont and Schaanning (2019)[2]. Moreover, with the same rationale in mind, we also model deleveraging needs according to a leverage adjustment speed parameter whose calibration is based on Duarte and Eisenbach (2021). This parameter captures the positive relationship between banks' deleveraging needs and realized asset sales. In this respect, depending on the severity of the fire-sale event, a bank

[2] Using a strict target-leverage constraint may push banks to be oversensitive to the binding constraint and leads to an overestimation of fire-sales spillovers when relatively small shocks hit banks' balance sheet. Thanks to this feature, banks are assumed to deleverage only when shocks push a bank's leverage above one-standard deviation of its historical leverage.

is assumed to adjust the speed at which it deleverages to spread the burden over time and in turn also reduce liquidation costs[3]. Complementary, banks are also assumed to deleverage due to a cash buffer target, which is bank-specific, and it is adjusted to account for bank-specific cash volatility preference. Hence, banks may deleverage to repay funding obligations, and to hold enough cash to withstand potential future liquidity shocks. In the end, we move away from a linear price-impact function and adopt a nonlinear approach leveraging upon Fukker et al. (2022)'s estimates for historical price dynamics[4]. In this respect, we show that banks' deleveraging process via fire sales tend to amplify shocks on average, but can also dampen them, and improve banks' regulatory ratios effectively. This result is consistent with Shin and White (2020), and Duarte and Eisenbach (2021) who highlight that banks can improve their post-shock leverage ratio depending on banks' starting conditions such as such as asset size, initial leverage, and asset holdings.

At the outset of the financial contagion literature, the focus was placed on the propagation of losses via cascade defaults and domino effects in the interbank market (Eisenberg and Noe, 2001). Although this contagion channel has been very predominant within the financial contagion literature, its relevance has decreased over time (Bardoscia et al., 2017). Furthermore, as noted by Glasserman and Young (2016), following the introduction of large exposure limits and collateral requirements, the likelihood of direct contagion through counterparty exposures has diminished in the banking system.

Beyond this set of methodological enhancements, we want to highlight few other important contributions to the literature. We design and calibrate a comprehensive set of regulatory thresholds triggering banks' failures and banks' management actions that the literature has acknowledged being lacking (Upper, 2011), and crucial to capture the unfolding of systemic stress events (Farmer et al., 2020; Aymanns et al., 2018; Lo, 2017; Armour et al., 2016).

There exist studies that rely on game theory, (Hałaj and Priazhkina,2021), or heuristics (Covi et al., 2019) to derive banks' responses conditional to imperfect information on other banks' actions and balance sheet positions. The former approach is beyond the scope of the paper, and we adopt a more heuristic-based approach triggering bank' management actions.

Overall, most of the literature focuses on modelling one financial contagion channel at time and used as trigger for the model dynamics a set of exogenous shocks which are not rooted into

[3] This assumption implies that banks won't be able to perfectly restore the initial target leverage constraint in the short-term.

[4] This non-linear calibration allows us to avoid over (under) estimation of fire-sale spillovers when small (large) size shock hit banks' balance sheet to achieve a more accurate estimate of the price impact and price mediated contagion as shown in Covi and Huser (2024).

an empirically calibrated probability distribution modelling risks stemming from banks' actual set of obligors and their intrinsic risks (actual borrowers' probability of default). Hence results are often abstracted from the actual features of the system, and do not have policy relevance. Contrary, our approach brings implications for the derived system equilibrium which, instead is a function of banks' heterogeneous starting balance sheet positions and overlapping and correlated portfolios of exposures via-a-vis the real economic and financial sector. Overall, the single-channel approach helps in studying and modelling comprehensively the features and dynamics of one risk dimension by isolating the effects. Nonetheless, it overlooks the importance of modelling the interactions and amplification effects across channels, thereby losing the complexity of the system's dynamics that may materialize under certain conditions (Eisenberg and Noe, 2001, Gai and Kapadia, 2010, Glasserman and Young, 2015; Caccioli et al., 2014, Cont and Schaanning, 2019). Very few papers aim to bridge this gap and, in this respect, our paper contributes to the stream of literature which deal with uncertainty and complexity as key modelling dimensions (Elsinger et al., 2006; Montagna et al., 2020; Covi et al., 2022, 2024; and Sydow et al., 2024).

*2.2 Result Contribution*

First, we provide estimates for the quantification of banks' default probabilities relying on a microstructural network-based methodology. Among the relevant papers of the microstructural and network literature, the only few examples to date, although with some differences in terms of methodology and data, are Elsinger et al., (2006) and Montagna et al. (2020), which provide respectively a systemic risk assessment for the Austrian banking sector, and the euro area banking sector. Contrary, in the market-based literature (Nagel and Purnanandam (2019), Brownlees and Engle, 2017; Adrian and Brunnermeier, 2016; Acharya et al., 2014), several models have achieved the quantification of financial institutions' probability of default. This substantial difference comes from the more complex, yet more granular approach of microstructural models that require confidential exposure data for their calibration, which often lacks a long time series dimension[5]. Our paper attempts to fill this gap since we back-test our model over a 10-year period with quarterly data and confront its output with market-based

[5] Microstructural models provide a more granular view since they are based on confidential information. They may also be better at identifying the impact of different channels of shock propagation, such as common exposures, fire sales or network effects (Gauthier et al., 2014). Nonetheless, they also have drawbacks in terms of calibration, model complexity, and replicability given they rely on confidential exposure data. This issue does not apply to market-based approaches since they exploit banks' equity and CDS prices which are available on a daily frequency and for more 20 years as of now.

approaches[6]. In this respect, we find that our average baseline PD estimates for the UK banking sector without feedback and amplifications tend to be aligned with market-based PD estimates. This is true especially in normal times, where estimates are respectively an average of 0.36% versus 0.39% during the period of the analysis. The main difference is found during period of stress and high market volatility (pandemic period) in which market-based estimates tend to overshoot materially our PD estimates even with feedback and amplification mechanisms. Overall, we find consistently with Van Oordt (2023) that market-based models tend to be much more sensitive to market uncertainty and stock price volatility. On the other side, microstructural models tend to be more anchored to structural slow-moving factors such as banks' balance sheet characteristics (capital and leverage ratios) and network of exposures, thereby avoiding overshooting. In this respect, we provide estimates for the impact of feedback and amplification mechanisms (especially fire sales) on the average bank default probability which account for 37% of total contribution (0.26% out of 0.7%), showing that the impact is heterogeneous and non-linear over time. This result corroborates findings from previous literature. Puhr and Schmitz (2014) calculate approximately 25% of the total loss in the solvency stress test stems from the asset fire sales; whereas Schmitz et al. (2019) show that incorporating this interaction results in additional 30% reduction of capital ratios.

Finally, we use the methodology as a policy laboratory in which a macroprudential policy assessment is carried out via counterfactual policy exercises as pointed out by Aikman et al. (2023), and Greenlaw et al. (2011). We assess the impact of the dividend restriction crisis tool (DR) introduced by the Bank of England (and other central banks) in 2020q1 to temporarily boost banks' capital during the pandemic period via the "retained earnings channel", given in periods of market disruption the "bank capital channel" is not a suitable option (Van den Heuvel, 2002). We find that this tool and channel was very effective in promptly keeping under control the stability of the UK banking system during a severe period of stress. This result complements previous findings in the literature (Acosta-Smith et al., 2023, and Dautović et al., 2023) which show a positive effect on lending, resilience and risk taking by banks. Nonetheless, alternative studies (Marsh, 2023; Matyunina and Ongega, 2022) find evidence that this tool may deteriorate banks' market valuation and in turn negatively affect their cost of funding, leading to counterproductive effects. We find that without a DR, the average bank default probability would have been higher by 32 bps (or 43%) between 2020 and 2021.

[6] We rely on banks' PD estimates estimated with the Eikon Starmine Credit Risk model which relies on a Merton model approach and banks' equity prices.

Moreover, the macroprudential effect is remarkable in terms of offsetting potential additional feedback and amplification mechanisms, which contribute 18 bps (56%) to the 32 bps increase. An equity market-based methodology would bring confounding results given DR breaks the negative relationship of CDS spreads and equity prices, turning it into a positive relationship in the short-term (lower stock prices and lower CDS spreads), consistently with findings from Dautović et al. (2023) and Acosta-Smith et al. (2023). Building upon this stress scenario exercise, we show how a macroprudential policy intervention aiming at lifting banks' capital base may contribute to reduce the average bank default probability. Other approaches have attempted to perform a calibration assessment of capital buffer requirements (Van Oordt, 2023; Coulier and Scalone, 2021), but none of them belong to the microstructural network literature, often relying on macro-econometric techniques.

## 3. Methodology

The methodology leverages upon the existing methodological contributions published in the stress testing, financial contagion, and network literature and combines them with a two-step procedure. Respectively, the first step consists in a stochastic approach modelling asset and funding shocks stemming from banks' counterparty defaults and the actual multiplex network of asset and funding exposures. Counterparty defaults are sampled according to a set of actual risk parameters (probability of default) which captures the prevailing state of macro-financial conditions across countries and sectors (non-financial corporates, non-bank financial corporates, credit institutions, governments) in each quarter[7]. Shocks are also modelled via a correlation structure capturing the dependence of shocks across countries and sectors, which are then transmitted to banks' balance sheet via the actual granular exposure network of banks' asset (loan and securities) as well as funding sources (deposits and repos). Asset and funding exposures from the household sector are also modelled with aggregated exposure data by country to obtain a full coverage of banks' balance sheet both on the asset and liability side.

Next, as a second step, we model feedback and amplification mechanisms deterministically as a function of banks' updated balance sheet position (after the transmission of shocks derived in step 1), and a set of empirically calibrated bank behavioural responses which are actioned according to the breach of bank-specific regulatory constraints (capital, leverage, and liquidity requirements) or deviations from historical bank-specific risk tolerance levels in terms of leverage ratio and liquidity preferences. This step allows us to capture the macroprudential

[7] This set of portfolio risk factors are estimated by banks on a quarterly frequency and submitted as part of supervisory COREP C.09 template.

system perspective which uncovers spillovers from aggregate risks stemming from the joint-interaction of banks' exposures to common shocks and bank-market responses to those shocks, which otherwise are invisible to microprudential supervisor as well as to the private bank itself.

### 3.1 Modelling Framework

**Figure 1** presents schematically the two building blocks of the methodology. We generate at STEP 1A the set of bank-quarter specific shocks on both the asset and liability sides of banks' balance sheet by sampling the default of counterparties banks are exposed to via loan and trading (bond and equity) book exposures and on the funding side via deposits and repo activities. This is consistent with Covi et al. (2022; 2024) and Sydow et al. (2024) approach. Thus, we obtain a simulation-specific (n=10.000) vector of defaulted counterparties for each quarter. Given each simulation's realized severity which is proxied by the amount of banks' exposures at default, we introduce banks' realized gross profits as inverse function of banks' exposures at default, i.e. the higher the system's realized stress, the lower banks' gross returns (interests, fee and commissions minus expenses) consistently with findings from Bolt et al., (2012) and Albertazzi and Gambacorta (2009).

Next, in STEP 1B we map the set of shocks according to a stock-flow consistent balance sheet-based approach and update the set of banks' balance sheet variables such as CET1 and TIER1 capital, total assets, risk weighted assets, cash on hands, and the regulatory ratios (CET1 and TIER1 capital, leverage, and liquidity ratios). Then we check whether banks have breached their regulatory ratios and accordingly we classify banks as viable if none of the constraints have been breached, or in distress when banks breach capital, leverage and liquidity buffer constraints, or in default[8] when they fall below minimum capital, leverage, and liquidity requirements. This approach is consistent with the existing literature as discussed in Halaj (2020). In the end, we update the network structure on both the asset and liability sides in order to account for the defaulted or withdrawn set of exposures.

This set of bank-specific states (viable, distress, default) is used to trigger banks' management actions as well as the market response, which are modelled deterministically and sequentially as part of STEP 2 in the form of feedbacks and amplification mechanisms. These behavioural responses and management actions are based on previous findings from the theoretical and empirical banking and financial contagion literature and calibrated on actual quarter and bank-

[8] Defaulted banks can be orderly or disorderly resolved as in Farmer et al. (2020). Orderly resolution (or liquidation) of a bank is a contagion-free, meaning that the bank becomes inactive, whereas disorderly includes rapid fire-sale (see Kok and Montagna, 2013). We choose the orderly path, as the regulatory body would want to minimize the costs of a bank failure.

specific balance sheet variables. It follows that the first dynamic response is captured via the channel defined as *bank-runs*, which is triggered when a bank breaches its CET1 capital buffer constraint or its leverage ratio distress constraint. In this respect, the market response implies that all financial institutions (banks and non-banks) start withdrawing short term funding categorized as sight deposits or do not roll-over short-term funding from repo operations, that is, they engage in precautionary withdrawals on the interbank market as explained in Davidovic et al. (2019), and Arinaminpathy et al. (2012). Overall, we assume that financial institutions act to manage their risk and choose not to lend out to stressed banks as shown in Acharya et al. (2022). Furthermore, this finding is also corroborated by empirical evidence in Blicke et al. (2022) who emphasize that the interbank market precisely identifies which banks will fail, and by Iyer and Peydró (2011) who find that banks do not liquidate interbank deposits from an average bank, but rather from those that have a high level of exposure to the failing and likely to fail ones. Moreover, healthy banks tend to also hoard liquidity as part of their risk aversion, meaning that banks observe others' liquidity hoarding behaviours and become more risk averse pushing them to reduce liquidity provision (Benzoni et al., 2015; Guisio et al. 2018).

**Figure 1**: Model Flow Diagram

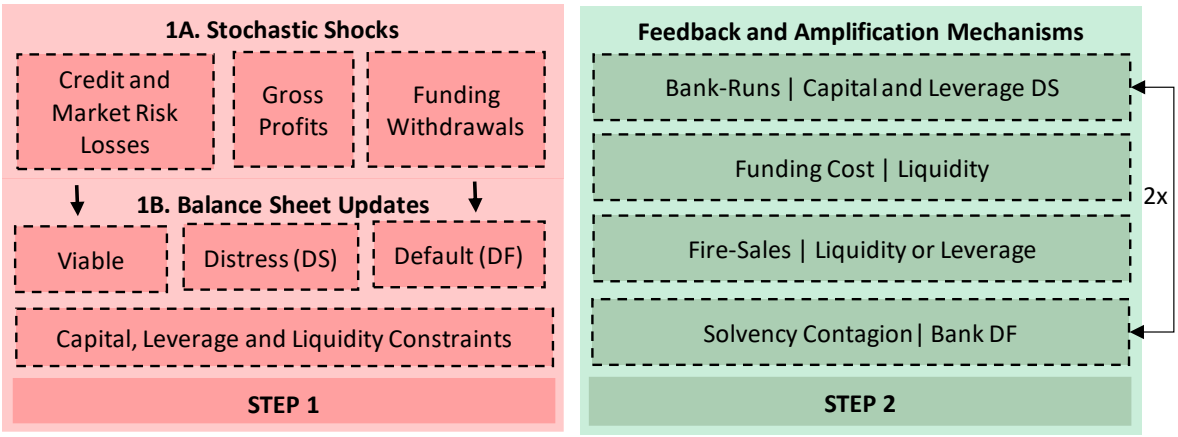


Note: Feedback and amplification mechanisms are modelled deterministically conditional to each bank's balance sheet position derived stochastically at STEP 1.

Accordingly, we model banks' liquidity management actions conditional to each bank's total funding needs as the sum of liquidity shocks experienced at STEP 1 and STEP 2 (bank runs). We then allow banks to engage in the secured and unsecured Sterling money markets to raise cash and in turn satisfy liquidity needs (offset liquidity shocks). In this respect, we model endogenously demand for funding and exogenously the supply of secured and unsecured funding conditional to the historical market size and to the bank-specific amount of high-quality liquid assets available to pledge (HQLA). Consistently we also model endogenously the cost of funding each bank pays as a function of: i) the central bank main refinancing rate

which is a time-varying parameter; ii) a bank-specific spread capturing the deteriorated solvency position (rating-based approach); iii) and a market spread capturing the level of stress in funding markets. Hence we compute a bank's total funding costs conditional to a specific liquidity stress horizon so as to model solvency-liquidity interactions stemming from liquidity shocks to solvency spillovers. The empirical literature have emphasized that a higher leverage (Annaert et al., 2010) and higher solvency risk (Pierret, 2014) lead to increased funding costs. Once this step is completed, we update the set of indicators tracking the stock and flows of banks' balance sheet variables, and we determine whether banks may have still pending funding needs or deleveraging needs. Funding needs may have been only partially satisfied given that the supply of secured and unsecured funding is constrained by the Sterling money market size and by the limited set of HQLA securities available to pledge, which is a subset of the overall portfolio of securities a bank holds. Instead, deleveraging needs may arise due to the set of credit and market risk shocks experienced at STEP 1 which may have led to a deterioration of a bank's leverage ratio. In this respect, the management action a bank is allowed to take is the sale of securities to satisfy the remaining funding needs and/or to restore the initial (target) leverage ratio (Duarte and Eisenbach, 2021; Bindseil, 2013, Van den End, 2010; Greenwood et al., 2015). The sales of assets take place at a discounted price which is derived using a heterogeneous security-specific price impact function whose price dynamics are modelled conditional to the asset-specific selling pressure and the market-specific severity of the fire-sale event - both features endogenously derived. Hence, we compute price-mediated contagion as marked-to-market (MtM) losses experienced by a bank on its holdings and sales of securities. This action may lead to a deterioration of a bank's solvency position via MtM losses, though under certain conditions it may also lead to an improvement in the bank's solvency-related regulatory capital and leverage ratios[9]. Contrary, the sales of assets always improve a bank's liquidity position.

Banks are assumed to de-leverage according to a targeted leverage ratio and to a leverage adjustment speed parameter (Greenwood et al., 2015) applying a pro-rata selling strategy. In the end, we update the set of banks' balance sheet variables, and model solvency contagion as credit risk losses stemming from interbank market exposures vis-à-vis the endogenously-

[9] For instance, keeping everything else equal, the composition of a security portfolio (low versus high share of risk assets) may determine whether the outcome results to be positive or negative. The sales of securities of a low-risk portfolio may not cause enough losses to reduce a bank's capital base more than the reduction in total assets and risk-weighted assets, leading the regulatory ratios to improve. Contrary a high-risk security portfolio tends to be conducive to a deterioration of regulatory ratios. Ceteris paribus in terms of portfolio composition, the overall outcome may vary also according to the level of market stress and selling pressure experienced in each simulation since the price of sales is determined endogenously by those two parameters.

derived set of defaulted banks. We repeat STEP 2 twice given that in our framework we model the deleveraging process consistently with a leverage adjustment speed parameter (Duarte and Eisenbach, 2021) which assume partial-deleveraging in each loop in order to avoid overestimation of fire-sale spillovers.

3.2 Stochastic Simulations

The model dynamics are triggered by an initial shock stemming from the defaults of banks' counterparties, respectively non-financial corporations (NFC), non-bank financial institutions (NBFI), credit institutions (CI) and governments (GG)[10]. Banks are exposed to this set of institutions on both sides of the balance sheet, respectively by providing loans and holding securities issued by these firms, and by obtaining fundings such as sight and term deposits as well as repo contracts from other credit institutions, NBFIs and non-financial corporates. In this respect, we randomly sample the vector of counterparty defaults using a Gaussian-Copula model with counterparty-specific (*j*) probability of default in period *t* ($PD_{j,t}$) as well as a dependence structure modelled by a correlation structure for country-sector pairs (Sydow et al. 2024; Covi et al. 2024). For technical details we refer the reader to these papers and to Appendix A. The counterparty-specific probabilities of defaults are time varying and reflect changes in macro-financial conditions, whereas the correlation structure is time-invariant capturing the historical dependence of macro shocks across country and sector pairs[11].

The stochastic defaults of counterparties lead to loan losses in bank *i*-s' portfolios and to market losses on their security holdings $\left(L_{i,n,t}\right)$ as well as to funding shocks $\left(F^{1}_{i,n,t}\right)$ in each scenario *n* and quarter *t*, given sight deposits are withdrawn to pay default-related obligations and repo activities are not rolled over. Hence, the vector of firm defaults captures the relationships between correlated asset and liability shocks on banks' balance sheet. This correlation depends on the degree of portfolio overlapping for both sets of counterparties on the asset and funding sides. The only sector for which we don't rely directly on the sampling method to estimate credit risk losses (given the lack of granular exposure data) is the household sector (HH). In this regard, we augment the model with loan losses stemming from mortgages and consumer credit relying on banks' aggregated loan amounts by country-sector and asset type. Consistently with Sydow et. al. (2024), when we consider an aggregate country-sector

[10] Contrary to Sydow et al. (2024), we extend the set of counterparty defaults to all sectors, instead of limiting it to NFC and a subset of NBFI.

[11] In Section 4 we provide more details on the calibration of this dependence structure. We highlight at this point that we rely on a time-invariant correlation structure instead of a time-variant since it is beyond the scope of this paper to model this source of variation. See Covi et al. (2022) for further insights.

exposure, we cannot sample individual default events. We rather model HH losses $\left(L_{i,n,t}^{HH}\right)$ consistently with a country-asset specific impairment rate whose relative severity across simulations is scaled according to the realized severity derived in the stochastic loss component. Hence, we assume that a higher number of counterparty defaults cause a higher stress in the household sector (higher impairment rate) which takes place via the unemployment channel. Similarly, we model funding shocks stemming from households' aggregated sight and short-term deposits by country and sector $\left(F_{i,n,t}^{HH}\right)$. Last, we introduce a vector of exogenous gross returns $\left(P_{i,n,t}\right)$ which is negatively correlated to the severity of the stochastic loss component (Bolt et al., 2012), and whose calibration relies on historical bank-specific net operating income data. We refer to Section 4 for technical details about the data and calibration. Overall, we obtain two vectors of shocks, respectively a profit and loss vector $\left(PL_{i,n,t}\right)$ - Equation 1a - and a funding shock vector $\left(F_{i,n,t}\right)$ - Equation 1b - which are used to derive 1-year ahead distribution of banks' balance sheets at time t.

$$PL_{i,n,t} = P_{i,n,t} - L_{i,n,t} - L_{i,n,t}^{HH} \quad (1a)$$

$$F_{i,n,t}^{1} = F_{i,n,t} + F_{i,n,t}^{HH} \quad (1b)$$

3.3 Balance Sheet Accounting

Banks' balance sheet variables are derived for *n* simulations conditional to the bank-specific vector of shocks, respectively solvency (PL) and liquidity shocks (F). Hence, the starting balance sheet position (S=0) of bank (*i*) at time (*t*) is updated accordingly to obtain balance sheet position post STEP 1 (S=1), i.e. post-shock. In this respect, we update banks' total assets ($TA_{i,n,t}^{1}$), risk weighted assets ($RWA_{i,n,t}^{1}$), cash ($CASH_{i,n,t}^{1}$), CET1 and TIER1 capital ($CET1_{i,n,t}^{1}$ $and$ $TIER1_{i,n,t}^{1}$), CET1 capital ratio ($CET1r_{i,n,t}^{1}$) and Leverage Ratio ($LR_{i,n,t}^{1}$) as well as the network of exposures, respectively loan network ($L_{i,j,n,t}^{1}$), security network ($S_{i,j,n,t}^{1}$), and the funding network ($F_{i,j,n,t}^{1}$) between bank *i* and counterparty *j*[12].

Table 1 summarizes the UK banking system's balance sheet composition and reports the relevance of each variable (as aggregate). In this respect, the PL shock affects the loan and security portfolios on the asset side and the capital base on the liability side. Contrary, a funding shock affect the deposit base of a bank on the liability side and simultaneously the cash base on the asset side. In this methodology we do not model derivatives on both sides of the balance

[12] Appendix B reports the technical details.

sheet as well as other assets and liabilities and short positions. Overall, we capture 86% of UK banks' assets and liabilities making our methodology well-representative.

Table 1 – Banking System's Stylized Balance Sheet Decomposition

| Assets | Liabilities |
|---|---|
| CASH (14%) | DEPOSIT (68%) |
| LOAN (54%) | |
| SECURITY (17%) | DEBT SECURITY (12%) |
| | DERIVATIVES (11%) |
| DERIVATIVES (6%) | OTHER FIN. LIABILITY (2%) |
| OTHER ASSETS (9%) | SHORT POSITION (1%) |
| | CAPITAL (6%) |

Source: Supervisory template FINREP F.01 and F.02.
Note: Values in brackets refer to share of total assets. Securities are split between Bond (14%) and Equity (3%) instruments. Other Assets such as investments in subsidiary and joint ventures, tangible (property, plant and equipment investment property) and intangible assets (goodwill and other intangible assets and intangible assets), current and deferred taxes, and non-current assets. Capital refers to own funds.

### 3.4 Regulatory Constraints: Default and Distress Thresholds

We model three states of a bank, respectively, viable, distress and default. A bank is viable when none of the constraints is breached. Contrary, a bank is in distress or default when it breaches regulatory capital, leverage and liquidity requirements, respectively buffer and minimum requirements.

*Default Conditions*

A bank is in solvency default if CET1 ratio is below CET1 minimum capital requirements which is calibrated to 7% of a bank's RWAs given additional Tier 1 instruments (AT1) get converted into CET1 capital once this threshold is breached.

A bank is in leverage default if a bank's leverage ratio is larger than 31 times (3.25%) its TIER1 capital[13]. A bank is in liquidity default if the sum of cash and stock of HQLAs falls below its liquidity needs.

*Distress Conditions*

A bank is in solvency distress if it breaches its CET1 capital buffer requirements which are set to 10% of RWAs.

A bank is in leverage distress if its leverage ratio is larger than 25 times its TIER1 capital.

A bank is liquidity distress if its cash buffer, capturing a bank's liquidity preference, falls below 0[14]. This set of states are used to trigger banks' management actions aiming at improving a

[13] Prior to mid-2016 this threshold was set to 33 (3%) as by Basel standards. In this respect, for comparability purposes across quarters we use a constant threshold throughout the entire period of analysis. For reference on leverage ratio calculation see PRA Rulebook.
[14] Appendix C reports the mathematical derivation.

bank's current state, as well as market reactions which may further deteriorate a bank's capital, leverage, and liquidity position.

## 3.5 Management Actions and Behavioural Rules

### *3.5.1 Bank Runs*

We introduce *bank runs* into the methodology by modelling short-term (1-month) funding withdrawals ($F_{i,n,t}^{BR}$) from the financial corporate and non-financial corporate sectors conditional to a bank's breach of its solvency or leverage distress thresholds (post STEP 1 shocks, $DS_{i,n,t}^{CET1}$ and $DS_{i,n,t}^{LEV}$) and proportional to the severity of the solvency shock experienced. This is the first solvency-liquidity interaction we introduce into the methodology. This set of market responses can be due to a precautionary motive, whose evidence was found during the 2008 GFC as in Berrospide (2021), and Acharya and Merrouche (2012), or to a speculative motive as found in Gale and Yorulmazer (2013) or due to a more generalized hoarding behaviour (Benzoni et al., 2015, Guisio et al., 2018). Hence this modelling feature influences the liquidity ratios as well as the leverage ratio since cash reserves are deducted from leverage exposures per leverage ratio calculation. Funding shock vector gets updated to values of $F_{i,n,t}^{2}$.

$$F_{i,n,t}^{2} = F_{i,n,t}^{1} + (F_{i,n,t}^{BR} \mid DS_{i,n,t}^{CET1} = 1 \; or \; DS_{i,n,t}^{LEV} = 1) \quad (2)$$

### *3.5.2 Secured and Unsecured Borrowing*

Once the vector of funding shocks ($F_{i,n,t}^{2}$) is computed, we allow banks to access the secured and unsecured money markets to potentially offset funding withdrawals (Bindseil, 2013). In this respect, we assume banks to target a minimum level of cash reserves ratio (as share of total assets), defined as target cash base ($Cash\_base_{i,t}^{T}$).This level is calibrated according to banks' historical cash ratio volatility ($\sigma_i^{Cash}$), which resembles banks' preference in using cash buffer to offset liquidity shocks ($Cash\_Buffer_{i,t}$).

$$Cash\_base_{i,t}^{T} = Cash_{i,t} - Cash\_Buffer_{i,t} \quad (3a)$$

$$Where: Cash\_Buffer_{i,t} = \frac{\sigma_i^{Cash}}{E[Cash_i]} * Cash_{i,t}$$

Hence, banks are assumed to implement funding management actions when the cash base is below the initial target, that is, when the cash buffer post funding shocks ($F_{i,n,t}^{2}$) turns negative. Hence, we derive the bank-specific demand for funding ($D_{i,n,t}$) as reported in Equation 3b.

$$D_{i,n,t} = Cash\_Buffer_{i,t} - F_{i,n,t}^{2} \;\; when \; Cash\_Buffer_{i,t} - F_{i,n,t}^{2} < 0 \quad (3b)$$

Next, demand for funding at a bank-level is satisfied via secured and unsecured borrowing and constrained by the size of the secured and unsecured markets (supply functions) as well as by

the amount of HQLA available to pledge for repo transactions. Hence, we derive supply functions for secured and unsecured funding consistently with findings from the relevant literature and calibrate the market size to be in the range of 80 to 130 billion £ on the secured market, and 36 to 48 billion £ on the unsecured market[15].

In this respect, Di Filippo et al. (2020) and DeFiore et al. (2017) provide evidence that a substitution effect exists between the demand for unsecured and secured funding: the latter increases and the former reduces in times of stress (when counterparty credit risk increases)[16]. The reduction of unsecured lending is motivated by the precautionary liquidity hoardings. The supply of the secured funding increases when the credit risk increases as banks perceive repos to be a safer transaction since it implies a collateralized operation (Nagel, 2016, Gorton, 2017). Reduced lending on the unsecured market is explained via also credit rationing, and refinancing is still possible on the secured market (Hoerova and Monnet, 2016). Besides the increased counterparty risk, decline of lending can be explained with declining trust among banks, as in Allen et al. (2020). Empirical data on the UK market is in line with these theoretical considerations. On the one hand, Hüser et al. (2024) showed that the volumes of the secured repo market increased during the *dash for cash* episode of 2020, with banks doubling their average daily cash lending, on the other hand Acharya and Merrouche (2012) provide evidence that the UK unsecured market collapsed during the 2008 GFC.

Hence, we first model in aggregate the supply and demand of liquidity in the (un)secured markets following Dehmej and Gambacorta (2019)'s approach, where the system supply depends on the amount of capital and deposits, alongside the market-specific interest spread ($spread_t^{(un)sec}$). Whereas the system demand depends on aggregated set of banks' total funding need ($\sum_i^I D_{i,n,t}$) and the interest spread.

$$S_{n,t}^{(un)sec} = a_t^{(un)sec} + b \cdot spread_{n,t}^{(un)sec},\ b > 0 \qquad (3c)$$

$$D_{n,t}^{(un)sec} = c_t^{(un)sec} - d \cdot spread_{n,t}^{(un)sec},\ d > 0. \qquad (3d)$$

We calibrate values *a*, *b*, *c*, and *d* for each quarter and realisation such that the resulting demand and supply functions at medians (normal times) and tail realisations (stress conditions) correspond to the observed historical volumes in the (un)secured UK markets. Hence, our

[15] See Appendix D for details about the calibration.

[16] To avoid reputational costs, banks try to avoid breaching the regulatory requirements (in line with the BoE and PRA Discussion Paper (DP) 1/22) despite HQLA having purpose of being usable in stress events (Duncan et al., 2022). Reason being that it could lead to a liquidity spiral where banks cannot access funding as before, and/or face greater funding costs.

approach captures the substitution effect taking place between the two markets in stress time (di Filippo et al., 2022; Piquard and Salakhova, 2019; and DeFiore et al., 2017). If the level and dispersion of risk are low, the unsecured interbank market operates smoothly (Heider et al., 2009). When risk increases, safer banks leave the unsecured market, and the interest rate rises to reflect the presence of riskier banks and a constrained supply. Furthermore, it also depends on the overall market-wide risk as described in Bechara et al. (2024). These features imply that the worse the funding shock realization, the higher is the demand for secured funding relative to the unsecured one[17]. The realized severity affects our supply curve.

Contrary, the demand curve is downward sloping at each realisation, both on the secured and unsecured market, with banks being price takers. We obtain optimal quantities and spreads on both markets where the supply and demand functions intersect by equating (3c) and (3d), in each quarter and each realisation: $S_{n,t}^{(un)sec\ optimal} = D_{n,t}^{(un)sec\ optimal}$.

These quantities on the system level are then distributed across banks by using individual demands for liquidity at bank level. We calculate the demand weights for each bank in each realisation by quarter and distribute the total secured and unsecured borrowing accordingly[18]. We so derive the bank-specific vector of realized quantities for secured ($B_{i,n,t}^{S}$) and unsecured borrowing ($B_{i,n,t}^{U}$). We so obtain the updated level of cash reserves ($Cash_{i,n,t}^{3}$):

$$Cash_{i,n,t}^{3} = Cash_{i,t} - F_{i,n,t}^{2} + (B_{i,n,t}^{S} + B_{i,n,t}^{U}) \quad (4)$$

### *3.5.3 Funding Costs*

The second solvency-liquidity interaction we introduce into the methodology is the modelling of the funding cost channel (FC) as a function of the quantity borrowed from secured and secured markets $(B_{i,n,t}^{S} + B_{i,n,t}^{U})$ and the cost of funding, i.e. the applied interest rate (CoF). The empirical literature finds an inverse relationship between banks' solvency position and the implied interest rate. Aymanns et al. (2016) on a large sample of US global banks find that solvency position is negatively related to funding costs, with wholesale funding cost being more sensitive to solvency position during stress time when compared to normal times, with the relationship being also non-linear. Similar evidence can be found in Hasan et al. (2016) covering a sample of 160 global banks. Higher solvency risk also limits the access of a bank to short-term funding, as found in Annaert et al. (2013), Babihuga and Spaltro (2014), and Pierret

[17] See Table D.3 in Appendix D.

[18] The weights are based on each bank's share of liquidity needs over total needs in the system. We also constrain the amount of secured borrowing according to the amount of HQLA assets available to pledge and deduct this quantity from the portfolio of securities.

(2015). When focusing on UK banks, Dent et al. (2021) found that a negative shock to banks' solvency position is associated with an increase in banks' marginal cost of wholesale funding. Authors confirm existence of a non-linear relationship between funding costs and solvency shocks: based on a threshold model, authors find that a deterioration in the leverage ratio of 100 bps can increase CDS premia (funding cost proxy) from 6.5 (low risk) to 30 basis points (high risk) on average. Other evidence of a non-linear relationship between solvency and funding costs is found in Schmieder et al. (2012) and BSBC (2013). Moreover, there is also evidence of a systemic factor influencing cost of funding as shown by Acharya and Merrouche (2012) who argue that borrowing rates depend on market conditions regardless of banks' counterparty risk.

Consistently with this set of stylized facts, we model the cost of funding (eq. 5) as a function of three main factors, respectively the central bank main refinancing rate ($CB_t$) which is quarter-specific, a systemic market component or market spread capturing the stress experienced in the funding market ($spread_{n,t}^{sys}$) across realisations (*n*), and a bank-specific component ($spread_{i,n,t}^{bank}$) capturing banks' deteriorated solvency position mapped according to their distance to default (DtD):

$$CoF_{i,n,t} = CB_t + spread_{n,t}^{sys} + spread_{i,n,t}^{bank} \quad (5)$$

The central bank main refinancing rate is observed at each quarter *t*. Then, the system spread for secured and unsecured markets is modelled in a non-linear way and is proportionate to the severity of funding shocks aggregated on a system level. System spreads relative to CB rate range from -10 (normal times) to +20 basis points in period of elevated stress (Covid) for the secured market and -4 to 22 bps for the unsecured market, which is based on historical data. The bank-specific spread is modelled as in Hałaj (2018), that is, based on a bank's deteriorated solvency position after the initial shock, i.e. CET1 ratio distance to default from minimum capital requirements such that the DtD is rescaled into additional 0 to 500 basis points, where 500 bps approximates an institution that is close to default[19]. Dynamics of both secured and unsecured values of CoF is shown in Appendix E.

After deriving the cost of funding for each bank (i) in each simulation (n), and at time (t) for secured and unsecured borrowing, we derive a bank's total funding costs ($FC_{i,n,t}$) over a 90 days stress scenario as follows:

$$FC_{i,n,t} = FC_{i,n,t}^{S} + FC_{i,n,t}^{U} \quad (6)$$

[19] This calibration is in line with findings in the literature (Bonfim and Santos, 2004; and Schmitz et al., 2017).

$$Where: FC^{S}_{i,n,t} = \left(B^{S}_{i,n,t} * CoF^{S}_{i,n,t}\right) * \frac{90\ days}{360} \;\; ; \;\; FC^{U}_{i,n,t} = \left(B^{U}_{i,n,t} * CoF^{U}_{i,n,t}\right) * \frac{90\ days}{360}$$

We re-update all banks' balance sheet accordingly (index 3) and the network of exposures.

### *3.5.4 Fire-Sales Mechanism*

Next, we introduce fire sale mechanics into the methodology which are designed to satisfy potential remaining liquidity needs, and to accommodate deleveraging needs due to a leverage ratio being above a bank's target leverage - the third solvency-liquidity interaction.

*Selling Pressure*

A bank aims to liquidate $Q^{*}_{i,n,t}$ of security holdings if the leverage ratio post shock ($LR^{3}_{i,n,t}$) is above its initial target leverage ($LR^{T}_{i,t}$). This level is calibrated according to banks' historical leverage ratio volatility ($\sigma^{Lev}_{i}$), which resemble banks' risk preference. This implies that if leverage ratio stays within this confidence band ($LR^{T}_{i,t}$ , $LR_{i,t}$) banks do not act. This feature is implemented to avoid banks being over-reacting to small shocks[20].

$$Q^{*}_{i,n,t} = TA^{3}_{i,n,t} - Cash^{3}_{i,n,t} - TIER1^{2}_{i,n,t} * LR_{i,t} \;\; if \;\; LR^{3}_{i,t} > LR^{T}_{i,t} \qquad (7)$$

Where: $LR^{T}_{i,t} = LR_{i,t} + \frac{\sigma^{Lev}_{i}}{E[Lev_{i}]} * LR_{i,t}$

Moreover, as discussed in Section 3.1, we model the deleveraging process consistently with a leverage adjustment speed which assume partial-deleveraging. As presented in Duarte and Eisenach (2021), we calibrate the leverage adjustment speed ($LaS_{i,n,t}$) to be in the range [12.5% - 35%] and positively related to the deleveraging needs ($Q^{*}_{i,n,t}$) a bank experiences, that is, the higher the needs, the faster the adjustment speed[21].

$$Q^{**}_{i,n,t} = \left(Q^{*}_{i,n,t} * LaS_{i,n,t}\right) \;\; with \;\; LaS_{i,n,t} \in \left[12.5\%_{n \in (1th\ decile)} - 35\%_{n \in (9th\ decile)}\right]$$

Afterwards, if a bank did not succeed to restore a non-negative cash buffer ($Cash\_Buffer^{3}_{i,n,t}$) via secured and unsecured borrowings, it may incur into asset sales to achieve that. Depending on whether the remaining funding needs are larger than deleveraging needs, the final quantity of assets sold ($Q^{***}_{i,n,t}$) by bank is determined as follows:

[20] We assume as in Cont and Schaanning (2019) and Covi and Huser (2024) among others that banks have imperfect information on asset price dynamics and sell $Q^{*}_{i,n,t}$ using current asset prices and not the realized ones post fire sales. This assumption is consistent with the price impact derivation, which is a function of security-specific selling pressures and market-selling pressures (or market stress), both being a function of total banks' asset sales.

[21] We map a bank's deleveraging need into deciles, and apply incremental steps to the adjustment speed of 2.5%, from 12.5% (lowest decile) up to 35% (top decile).

$$Q^{***}_{i,n,t} = Q^{**}_{i,n,t} \;\; if \;\; Q^{**}_{i,n,t} > \left|Cash\_Buffer^{3}_{i,n,t}\right| \;\; otherwise \; Q^{***}_{i,n,t} = \left|Cash\_Buffer^{3}_{i,n,t}\right|$$

Finally, to determine the quantity of each security (s) to be sold ($Q^{***}_{i,s,n,t}$) we assume that banks rely on a pro-rata approach, that is, a proportional allocation across all securities in a firm's portfolio (Covi and Huser, 2024). This approach is also corroborated by Jiang et al. (2021) and Schaanning (2016) that suggest that a pro-rata approach is more suitable for periods of stress. Finally, we derive the total market selling pressure ($Q^{M}_{n,t}$) by summing across banks the realized bank-specific selling pressure ($Q^{***}_{i,n,t}$):

$$Q^{M}_{n,t} = \sum_{i}^{I} Q^{***}_{i,n,t}$$

*Price Impact Function*

Once we have determined the quantity sold for each security ($Q^{***}_{i,s,n,t}$), we rely on heterogeneous price impact functions to derive the security-specific price change $p^{*}_{s,n,t}$. In this respect, the literature has used multiple approaches, homogeneous versus heterogeneous price functions calibrated on a security or asset-class level. One of the most common approaches is Cont and Wagalath (2016) which derives a price change conditional to the volumes sold and the depth of the market for the asset (s)[22]. We follow Covi and Huser (2024) and rely on Fukker et al. (2022) who estimate non-linear price impact functions via quantile regression for a wide range of securities (bond and equity) with heterogeneous characteristics[23]. Moreover, conditional to the characteristic of the security, the price impact varies as a non-linear function of the security-specific volume sold (£10, 50, 100 million) and according to the severity of the fire-sale events (ranked by percentiles)[24] . Hence, we borrow from Fukker et al. (2022)'s the set of security-specific price impact functions ($F_s$) and we match them to our set of securities (s) according to the above described characteristics. For each $F_s$ we determine the realized price impact according to i) the estimated security-specific total selling pressure ($Q^{*}_{s,n,t}$ ) summing

[22] Calibrating the market depth on a security-level across time is data intensive and not feasible to extend to a large number of securities. Moreover, this approach does not consider how price changes are affected non-linearly conditional to the severity of the fire-sales. For this set of reasons,

[23] Respectively by issuing sectors (NFC, GG, FC, CI) and country as well as by rating (low, medium, high) and size of the firm (small, medium, large).

[24] For each security the price impact also depends on the percentile of the historical price change distribution, which we model via the market selling pressure.

across all banks and ii) the estimated Market Selling Pressure ($Q^{M}_{n,t}$) whose severity is determined by its percentile compared across simulations and quarters[25].

$$p^{*}_{s,n,t} = F_s\left(Q^{***}_{s,n,t} \ , \ Q^{M}_{n,t}\right) \quad (8)$$

*Fire-Sale Losses*

As last step, we derive Mark-to-Market losses ($FS_{i,n,t}$) for each firm i's portfolio of security in each simulation (n) and time period (t). In this respect, we both compute direct ($FS^{D}_{i,n,t}$) and indirect losses ($FS^{Ind}_{i,n,t}$) respectively on the security sold as well as on the remaining securities in firms' portfolios.

$$FS_{i,n,t} = FS^{D}_{i,n,t} + FS^{Ind}_{i,n,t} \quad (9)$$

$$Where: \ FS^{D}_{i,n,t} = \sum_{s}^{S} Q^{***}_{i,s,n,t} * p^{*}_{s,n,t} \quad and \quad FS^{ind}_{i,n,t} = \sum_{s}^{S} Q^{P}_{i,s,n,t} * p^{*}_{s,n,t}$$

In the end, we re-update all banks' balance sheets accordingly (index 4). Specifically, the generated liquidity from asset sales go to increase a bank's cash reserves (which are exempted from leverage exposure calculation) and thus affects positively (reduce) the leverage ratio, thereby counterbalancing the negative impact from fire-sale losses which reduce the capital base - denominator of the leverage ratio. Depending on whether the numerator (asset exposures) decreases faster than the denominator (Tier 1 capital), the leverage ratio may improve or further deteriorate post fire-sale dynamics. We test this feature in the sensitivity analysis section by performing a counterfactual policy exercise. Among the key factors affecting the positive/negative variation in the leverage ratio, banks' portfolio composition plays a crucial role. In fact, the higher the share of risky assets and the higher the price impact experienced, the faster the decrease in the denominator (Tier 1) relative to the numerator (TA). The leverage ratio is not the only regulatory ratio that is affected by the deleveraging process. It may also contribute to reduce the bank's stock of risk weighted assets which is used to derive the CET1 capital ratio (CET1 / RWA). In this respect, we acknowledge this channel and we adjust the stock of RWAs by the quantity of assets sold ($Q^{***}_{i,n,t}$) multiplied by the share of RWAs over total assets which is adjusted by the share of risky assets over total assets (1-HQLA share) given HQLAs have 0 risk weights. In the end, we re-update all banks' balance sheet accordingly (index 5) and the network of exposures.

[25] The relative severity of market selling pressure which approximates the severity of the fire-sale event is compared across quarters since the total selling pressure in the 99th percentile during the pandemic period (2020-2021) is way larger than the total selling pressure for the 99th percentile during normal times (post pandemic), which is close to the 80th percentile of the pandemic period.

### *3.5.5 Interbank Contagion*

As last step, we consider the potential effects of solvency contagion via interbank exposures conditional to an institution being insolvent or illiquid. The solvency contagion channel has been always considered as one of the main channels of risk propagation in the interbank market since it accounted for a large share of interbank losses in the 2008 GFC (Glasserman and Young, 2016). Nonetheless, Bardoscia et al. (2017) has more recently identified a long-term decline in the contagion role played by this channel as we find. Hence, we rely on the standard Eisenberg and Noe (2001)'s approach to estimate potential losses ($SC_{i,n,t}$) on interbank exposures ($INT_{i,j,n,t}$) given counterparty bank j being in default ($Y_{j,n,t} = 1$).

$$SC_{i,n,t} = \sum_{j}^{J} INT_{i,j,n,t} * LGD_{i,j,n,t} * \ Y_{j,n,t} \ \ where \ Y_{j,n,t} = 1 \tag{10}$$

### *3.6 Simulation Steps*

As described in Section 3.1, we repeat the management action cycle presented in Section 3.5 twice given that in our framework we model the deleveraging process consistently with a leverage adjustment speed assuming partial-deleveraging (Duarte and Eisenbach, 2021). Thus, we calculate the sum of two rounds of funding costs, fire sale costs and solvency contagion costs as follows:

$$FC_{i,n,t} = \left(FC_{i,n,t}^{R1} + FC_{i,n,t}^{R2}\right); \ FS_{i,n,t} = \left(FS_{i,n,t}^{R1} + FS_{i,n,t}^{R2}\right); \ SC_{i,n,t} = \left(SC_{i,n,t}^{R1} + SC_{i,n,t}^{R2}\right).$$

Other approaches in the literature rely exclusively on one single cycle of management actions or asset liquidations given the first-round accounts for the majority of fire-sales spillovers (Caccioli et al. 2024). Ramadiah et al. (2022) also shows that conditional to a leverage targeting approach, one round seems to be the optimal approach. Contrary, Sydow et al. (2024) implement multiple rounds, although they show that most of the effects take place within the first two rounds of asset liquidation.

### *3.7 Model Outputs*

At this point, we are in the position to derive a profit and loss distribution $\left(PL_{i,n,t}^{PMA}\right)$ comprehensive of credit and market risk losses, augmented with net operating income, and amplified by solvency-liquidity interactions and financial contagion, that is, post banks' management actions (MA). Leveraging upon the stochastic approach, the aim is to study the severity and probability of tail outcomes affecting the UK banking sector. We thus aggregate the $PL_{i,n,t}^{PMA}$ across banks to obtain a $PL_{n,t}^{PMA}$ at the system level and so derive a Conditional

Capital at Risk measure ($CCaR_t^x$) tracking tail risk developments proxied by value at risk at the 99th, 95th and 90th percentiles of the distribution.

$$PL_{i,n,t}^{PostMA} = \left(P_{i,n,t} - L_{i,n,t} - L_{i,n,t}^{HH}\right) - (FC_{i,n,t} + FS_{i,n,t} + SC_{i,n,t}) \quad (11a)$$

$$PL_{n,t}^{PostMA} = \sum_{i}^{I} PL_{i,n,t}^{Post-MA} \quad (11b)$$

$$CCaR_t^x = \left[PL_{n,t}^{PostMA} \mid n \in (99^{th}, 95^{th}, 90^{th})\right] \quad (11c)$$

Moreover, we also define the Conditional Liquidity at Risk measure ($CLaR_t^x$) tracking the total amount of potential funding outflows ($TFO_{i,n,t}$) proxied by value at risk at the 99th, 95th and 90th percentiles of the distribution. Total funding outflows are derived as the sum of pre-bank-run funding withdrawals ($F_{i,n,t}^{BR1}$), funding withdrawals from bank-runs in the first round ($F_{i,n,t}^{BR2}$), and banks-runs taking place in the second round ($F_{i,n,t}^{3}$). We scale this output variable by the cash base and other liquidity measures to assess its size in relative terms.

$$TFO_{i,n,t} = \left(F_{i,n,t}^{1} + F_{i,n,t}^{BR1} + F_{i,n,t}^{BR2}\right) \quad (12a)$$

$$TFO_{n,t} = \sum_{i}^{I} TFO_{i,n,t} \quad (12b)$$

$$CLaR_t^x = \left[TFO_{n,t} \mid n \in (99^{th}, 95^{th}, 90^{th})\right] \quad (12c)$$

Nonetheless, from a financial stability perspective $CCaR_t^x$ is not an exhaustive indicator since an assessment of the system's fragility needs to be carried out by comparing potential tail outcomes against banks' capital and liquidity positions. In this respect, given we also derive consistently with $PL_{i,n,t}^{PMA}$ a full distribution of banks' balance sheet variables (CET1 ratio, leverage ratio and liquidity ratio), we can compute banks' default probability in terms of insolvency and illiquidity against regulatory default thresholds described in Section 3.4[26].

We so derive 1-Year ahead default probability of the banking system ($PD_t$) by multiplying each bank's default probability ($PD_{i,t}$) by a vector of time-invariant bank weights ($w_i$) measured as the average bank's share of total assets of the system over the period of analysis[27].

[26] See Appendix C for more details.

[27] We opt for a weighted average instead of a simple average to control for bank heterogeneity since within our sample of banks, the largest bank (HSBC) has 25 times the asset size of the smallest bank (Virgin Money). Moreover, we use a vector of constant weights to remove noise stemming from weights varying over time.

$$PD_{i,t} = \sum_{n}^{N} \frac{Y_{i,n,t}}{N} \; where \; Y_{i,n,t} = 1 \; if \begin{cases} CET1r_{i,n,t} < 7\% \\ LR_{i,n,t} > 31 \\ LIQ_{i,n,t} < 0 \end{cases} \quad (13a)$$

$$PD_t = \sum_{i}^{I} PD_{i,t} * \; w_i \; where \; w_i = E\left[\frac{TA_{i,t}}{\sum_i^I TA_{i,t}}\right] \quad (13b)$$

## 4 Data and Calibration

The model is estimated on a sample of seven major UK banking groups capturing £6.289 billion of total assets as of Q1 2024 and spanning over 37 quarters between Q1-2015 and Q1-2024[28]. No study in the stress testing and related financial network literature has been capable to estimate and test a microstructural model on a such long time-series dimension, usually limiting the analysis to a specific snapshot date. This represents a key contribution of the paper and allows to compare the model outputs consistently across quarters exploiting variation in banks' loan and security exposures as well as banks' balance sheet characteristics.

Table 2 reports summary statistics averaged across quarters for the set of banking groups subject to the analysis and aggregated at the level of the banking system. The upper section of the table shows the set of key regulatory ratios which also represent the starting positions of the analysis. The lower section of the table shows statistics for the networks of exposures (as ratio over total assets) which we use to model the propagation of shocks between bank i and counterparty j (obligor basis). Specifically, the portfolio of securities composed by bond and equity instruments range between 10% and 12% of banking system's total assets, of which half of the share is made of HQLA assets. Of similar size is the portfolio of corporate loan, while loan exposures to households (HH) range between 23% and 27% of total assets[29].

On the liability side, total funding ratio represents the share of withdrawable deposits such as sight deposits, deposits with agreed maturity below 1 month or repo transactions with maturity below 1 month[30]. It ranges between 47% and 54% of total assets, of which roughly 29% is made of corporate funding exposures between counterparty j and bank i, and the remaining share by deposits from the household sector. Security, loan and funding exposures are mapped on a counterparty basis identifying the sector issuing the security or underwriting the

[28] The sample of banking groups is made of HSBC, Barclays, Lloyds, NatWest, Standard Chartered, Santander UK, and Virgin Money.

[29] As part of the exposure asset network we also track for modelling solvency contagion spillovers interbank exposures among the sample of banks which represents a very small share of total asset in the system.

[30] We use 1-month has cutoff threshold to be consistent with a 30-days liquidity stress horizon (LCR assumption).

loan/funding contract, and the country of domicile[31]. Given these qualitative attributes on the counterparty, we assign a probability of default parameter to each obligor using a 1-Year probability of default (PD) by country and sector, and loss given default parameters (LGD) to each asset exposure. This set of risk factors are estimated by the banks themselves; they are time-varying on a quarterly basis and are reported as part of COREP 09 supervisory data. In the end, we want to highlight that the leverage ratio in the UK regulatory framework since mid-2016 has excluded from the calculation of the total exposure measure those assets constituting claims on central banks to facilitate the implementation of monetary policies at a time of exceptional macroeconomic circumstances. Consistently, the minimum LR requirements have been recalibrated to 3.25% instead of 3% (or ~31). As discussed in the methodology section and in Appendix B, we use the UK leverage framework over the entire period of analysis (also prior to mid-2016 for comparability purposes)[32].

Table 2 – Banking System's Summary Statistics

| **Balance Sheet Variables** | **2015** | **2016** | **2017** | **2018** | **2019** | **2020** | **2021** | **2022** | **2023** | **2024** |
|---|---|---|---|---|---|---|---|---|---|---|
| Total Assets (£ Billion) | 5435 | 5606 | 5304 | 5344 | 5625 | 6117 | 5928 | 6550 | 6332 | 6289 |
| RWA ratio (TA) | 36.8% | 33.8% | 32.9% | 31.5% | 30.1% | 27.4% | 26.7% | 26.5% | 27.0% | 27.3% |
| CET1 ratio (RWA) | 11.8% | 12.8% | 14.0% | 14.1% | 14.2% | 15.1% | 15.8% | 14.1% | 14.3% | 14.3% |
| TIER1 ratio (RWA) | 14.1% | 15.4% | 17.0% | 17.3% | 17.3% | 18.0% | 18.9% | 16.7% | 17.0% | 16.9% |
| Leverage ratio | 18.0 | 17.9 | 16.2 | 16.4 | 17.5 | 18.0 | 16.8 | 19.3 | 18.8 | 18.9 |
| Leverage ratio Incl. Cash | 19.3 | 19.3 | 17.9 | 18.3 | 19.2 | 20.3 | 19.8 | 22.7 | 21.8 | 21.7 |
| Cash ratio (TA) | 6.5% | 7.2% | 9.8% | 10.3% | 9.1% | 11.4% | 15.1% | 14.8% | 13.7% | 13.0% |
| Cash Buffer ratio (TA) | 1.3% | 1.3% | 1.8% | 1.9% | 1.7% | 2.2% | 3.0% | 2.9% | 2.6% | 2.5% |
| Security Portf. Ratio (TA) | 11.6% | 11.2% | 11.9% | 11.8% | 11.2% | 10.9% | 12.8% | 12.1% | 12.1% | 12.1% |
| HQLA ratio (TA) | 5.8% | 5.6% | 5.9% | 5.9% | 5.6% | 5.1% | 5.3% | 4.8% | 5.1% | 5.3% |
| Corp. Loan ratio (TA) | 13.0% | 12.5% | 13.2% | 13.1% | 12.5% | 11.4% | 11.6% | 10.8% | 10.7% | 10.8% |
| HH. Loan ratio (TA) | 26.1% | 25.2% | 26.6% | 26.4% | 25.1% | 23.4% | 24.8% | 23.5% | 24.1% | 23.8% |
| Interbank Exp Ratio (TA) | 0.01% | 0.01% | 0.01% | 0.01% | 0.01% | 0.02% | 0.01% | 0.01% | 0.02% | 0.01% |
| Total Funding ratio (TA) | 48.9% | 47.3% | 50.0% | 49.6% | 47.2% | 46.2% | 53.7% | 51.6% | 49.6% | 48.9% |
| Corp. Funding ratio (TA) | 27.8% | 26.9% | 28.4% | 28.2% | 26.8% | 25.4% | 29.7% | 29.1% | 29.4% | 29.4% |
| HH.Funding ratio (TA) | 21.1% | 20.4% | 21.6% | 21.4% | 20.4% | 20.8% | 24.0% | 22.4% | 20.2% | 19.5% |

Source: Supervisory COREP and FINREP data, and stress testing data.
Note: In brackets we report the denominator used for computing the ratio. Funding variables refer to the share of funding that can be withdrawn at sight or with a maturity below 1 month. HQLA ratio does not consider cash reserves, but only high-quality liquid securities.

[31] Respectively, non-financial corporates (NFC), non-bank financial corporates (FC), credit institutions (CI), and Governments (GG). For countries, we map exposures to counterparties domiciled in 135 countries.
[32] See Bank of England (2017) for more details on the UK leverage ratio framework. This policy change has indeed affected banks' cash preference over other type of liquid assets. Cash reserves as share of total assets increased materially between 2016 and 2024 (post introduction) passing from 7.2% to 13%.

## 5 Results

### 5.1 Realized Shock Distribution

We find that over time the UK banking system may experience on average with 1% probability (CCaR99) £95 billion of losses within one year horizon, whereas £35 billion with 5% probability tracked by CCaR95 index (**Figure 2**). The peak was reached during the Covid-19 pandemic (2020-21) at £117 billion, and since then tail risk severity materially reduced, with CCaR99 down to 79 billion in 2024q1[33]. As shown in Table 3a, this trend is even more marked when we look at the 95$^{th}$ and 90$^{th}$ percentile of the P&L distribution, the latter turning even positive in 2023-24 benefiting from higher interest rates and related increased in banks' operating margin. Overall, the system's expected outcome is £16 billion of average profits over time and £27 billion in 2024q1.

**Figure 2**: Tail Risk Developments

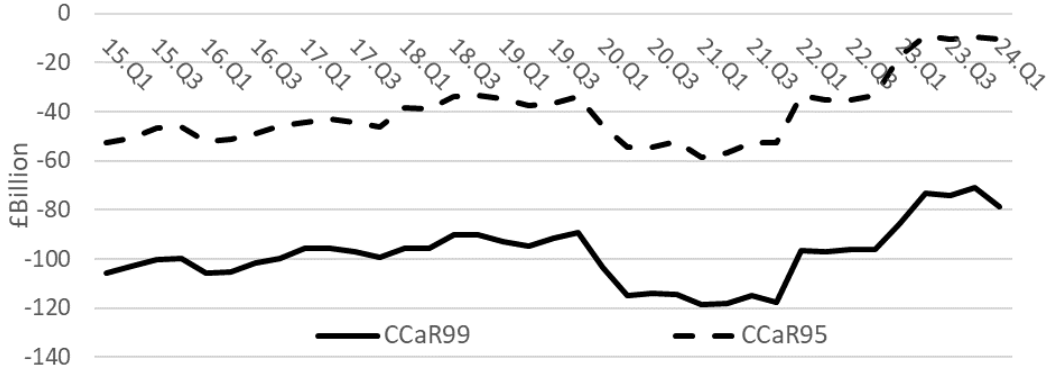


Note: CCaR refer to Conditional Capital at Risk for the 99$^{th}$ and 95$^{th}$ percentiles.

### 5.2 Decomposition of the results

As we combine multiple financial contagion channels and model the interaction between solvency and liquidity risks in a correlated manner that contribute to the overall tail risk developments, we decompose the results in this section.

Digging into the drivers of tail risk, as reported in Table 3b, we find that the reduction in tail risk is due to a material improvement in the generation of operating income (ECP), increasing from £9 billion in 2021 to £26 billion in 2024, to a material reduction in potential fire-sales spillovers, passing from £37 billion to £19 billion in the same period, and a slight decrease in credit and market risk losses (ECL), down to £86 billion. Most of the spillover effects stemming

[33] Although CCaR99 estimates are not directly comparable to the Bank of England's stress results given the former is based on prevailing quarter-specific macro and financial conditions, and the latter is based on a specific stress scenario, our loss estimates do not fall far from ACS results especially when macro-financial conditions deteriorate (pandemic period). The BOE's 2022-23 ACS stress test exercise estimates roughly £136 billion of losses taking place within the first year of an adverse stress scenario. The sample of banks is the same.

from management actions take place within Round 1 (67%) as shown in Table G1 in Appendix G**,** consistently with findings in previous studies.

Furthermore, we find that the fire-sale channel is the most relevant feedback and amplification channel at play, with an average impact at 99$^{th}$ percentile of £23 billion of losses (explain 18% of total variation). The impact varies materially over time between 15% and 28% depending on banks' security portfolio composition, on banks' starting leverage ratio and cash reserve positions, as well as on the severity of solvency shock distribution which is a function of the prevailing quarter-specific macro-financial conditions. Puhr and Schmitz (2014) calculate approximately 25% of the total loss in the solvency stress test stems from the asset fire sales; whereas Schmitz et al. (2019) show that incorporating this interaction results in additional 30% reduction of capital ratios. Similarly, Covi et al. (2024) find that fire sale losses conditional to VaR99 may account for 33% of total banks' losses.

Table 3a: Tail Risk Developments

| | 2015 | 2016 | 2017 | 2018 | 2019 | 2020 | 2021 | 2022 | 2023 | 2024 | AVG |
|---|---|---|---|---|---|---|---|---|---|---|---|
| CCaR99 | -95 | -97 | -91 | -93 | -92 | -112 | -117 | -96 | -76 | -79 | -95 |
| CCaR95 | -38 | -40 | -35 | -36 | -36 | -52 | -55 | -34 | -12 | -10 | -35 |
| CCaR90 | -9 | -13 | -7 | -7 | -7 | -20 | -26 | -1 | 8 | 7 | -7 |
| AVG | 16 | 12 | 13 | 14 | 16 | 11 | 8 | 18 | 28 | 27 | 16 |

Note: CCaR refer to Conditional Capital at Risk for the 99$^{th}$ , 95$^{th}$ and 90$^{th}$ percentiles, where AVG reports the mean value of the distribution.

Digging into the drivers of fire-sale (FS) losses, we find the highest severity take place over 2021-22 (~£36 billion), although the severity of the P&L shock reaches its peak in 2020 (£88 billion), much higher than £80 billion in 2021 and £60 billion in 2022. This may seem to be counterintuitive at a first glance given that deleveraging needs and in turn Fire-sales are positively related to the severity of the P&L shock via changes in banks' capital base and leverage ratios. Indeed, FS sales for the 99$^{th}$ percentile are higher by 10% in 2020 (~£460 billion) than in 2021-2022 (~£420 billion) given the higher P&L shock. FS losses being higher in 2021-22 than in 2020 can be explained by the change in the allocation of banks' security portfolios towards more risky assets with a higher potential downside risk and price impact in 2021 and 2022 relative to 2020. The average portfolio risk per unit of security exposure which proxies the potential downside risk of a security portfolio in terms of expected MtM losses decreases from -1.5% in 2020 to -0.8% in 2024q1. With rising interest rates and the related rising bond yields, banks started to invest more into HQLA and government bonds over 2023 and 2024, thereby reducing their portfolio risk and in turn the potential impact from FS losses.

Table 3b: CCaR99 Decomposition by Channel

| CCaR99 | 2015 | 2016 | 2017 | 2018 | 2019 | 2020 | 2021 | 2022 | 2023 | 2024 | AVG |
|---|---|---|---|---|---|---|---|---|---|---|---|
| ECL | -92 | -90 | -86 | -89 | -89 | -99 | -89 | -76 | -79 | -86 | -87 |
| ECP | 17 | 12 | 13 | 14 | 15 | 11 | 9 | 16 | 26 | 26 | 16 |
| P&L | -75 | -78 | -72 | -75 | -74 | -88 | -80 | -60 | -53 | -60 | -71 |
| FC | -0.5 | -0.4 | -0.2 | -0.2 | -0.2 | -0.2 | -0.1 | -0.2 | -0.3 | -0.4 | -0.3 |
| FS | -19 | -19 | -18 | -18 | -18 | -24 | -37 | -36 | -23 | -19 | -23 |
| SC | -0.04 | -0.05 | -0.03 | -0.04 | -0.03 | -0.08 | -0.04 | -0.05 | -0.02 | 0.00 | -0.04 |
| P&L PMA | -95 | -97 | -91 | -93 | -92 | -112 | -117 | -96 | -76 | -79 | -95 |

Note: CCaR is decomposed by channel respectively, credit and traded risks (ECL), gross profit (ECP), funding costs (FC), fire sales spillovers (FS) and solvency contagion (SC).

Looking at the contribution of the remaining channels, funding costs (FC) have a limited impact in the range of £100 to £500 million. This severity is a function of the size of the liquidity shock the system experiences, the main refinancing rate prevailing in that period, and the stress horizon assumed (90 days). In this respect, the highest impact takes place in 2015 and in 2024, though due to different drivers. In 2015 the main driving forces were the lower level of banks' liquidity position jointly with a lower level of banks' capital position (which affect the severity of bank runs), and a higher severity/size of potential funding withdrawals relative to 2024. As shown in Table 4, we estimate that in 2015 funding shocks in the 99$^{th}$ percentile are 10% of the total funding shock base (potential withdrawable deposits) or £270 billion instead of 6% in 2024 (£185 billion)[34]. Moreover, cash reserves were much lower in 2015 relative to 2024 (Table 2), and this reduces the funding shock ratio as share of cash reserves (CASH) from 76% to 23%. Contrary, the interest rate applied to the amount of liquidity borrowed is higher in 2024 than in 2015, consistently with a higher central bank refinancing rate, thereby pushing up the marginal cost of funding. Overall, the UK banking system seems to be less prone to fundings shocks and better insured thanks to the build-up in cash reserves over the period of the analysis. To benchmark our estimates, we provide two relevant comparisons. CLaR99 estimates are roughly 20-30% the size of the estimated liquidity outflows entailed in the liquidity coverage ratio regulation (LCR) for the same sample of banks and time periods. The difference is due to the LCR denominator being estimated conditional to a 30 days liquidity stress scenario, whereas our estimates, although calibrated to match the same length of the stress horizon (30 days), are measured as VaR99 according to the prevailing macro-financial conditions in that quarter[35]. Moreover, comparing our estimates with the historical example of the 1931 German banking crisis (Blicke et al. 2024) whose average run-off rate was estimated to be in the range

[34] Banks runs account on average for 1/3 of total funding withdrawals.

[35] We show in the next section 6.3 that our CLaR99 estimates conditional to a stress scenario resembling a GFC-type indeed get very close to the LCR assumption on funding outflows.

10%-20% given a 90-days stress horizon, we can state that our CLaR99 is well representative of a severe case of bank runs[36]. The key difference resides in the average HQLA share the German banking system held at that time, which amounted to 5% of total assets (Blicke et al. 2024), much lower compared to the UK banking system's share of cash and HQLA securities which averages around 16% of total assets (Table 2). The merit of this improvement in the numerator of the liquidity coverage ratio (HQLA) is certainly due to the introduction via Basel III standards of stricter liquidity requirements as the LCR itself entails.

Table 4: Funding Shocks Metrics

| Funding Shocks (VaR99) | 2015 | 2016 | 2017 | 2018 | 2019 | 2020 | 2021 | 2022 | 2023 | 2024 |
|---|---|---|---|---|---|---|---|---|---|---|
| Funding Shock Base (TA) | 49% | 47% | 50% | 50% | 47% | 46% | 54% | 52% | 50% | 49% |
| Funding Shock Ratio (FB) | 10% | 10% | 7% | 7% | 7% | 9% | 9% | 7% | 6% | 6% |
| Funding Shock Ratio (CASH) | 76% | 64% | 37% | 35% | 35% | 37% | 30% | 25% | 22% | 23% |
| Funding Shock Ratio (CASH+HQLA) | 40% | 36% | 23% | 22% | 21% | 25% | 22% | 19% | 16% | 16% |
| Funding Shock Ratio (CASH+SEC) | 27% | 25% | 17% | 16% | 15% | 18% | 16% | 14% | 12% | 12% |
| Net Cash Outflows (CASH) | 15% | 16% | 13% | 12% | 10% | 10% | 8% | 11% | 10% | 9% |
| Net Cash Outflows (CASH+HQLA) | 8% | 9% | 8% | 7% | 6% | 7% | 6% | 9% | 7% | 6% |
| Net Cash Outflows (CASH+SEC) | 5% | 6% | 6% | 5% | 4% | 5% | 4% | 6% | 5% | 5% |
| Net Liquidity Outflows (CASH) | 83% | 70% | 43% | 42% | 41% | 43% | 38% | 28% | 26% | 26% |
| Net Liquidity Outflows (CASH+HQLA) | 44% | 39% | 27% | 26% | 26% | 30% | 28% | 21% | 19% | 18% |
| Net Liquidity Outflows (CASH+SEC) | 30% | 27% | 20% | 19% | 19% | 22% | 21% | 15% | 14% | 13% |

Note: Net cash outflows refer to the net change in cash reserves after borrowing from the interbank market, whereas net liquidity outflows variable takes into account also the reduced value of banks' security portfolios.

In the end, we show in **Table G1** in Appendix G that the severity of funding shocks is positively correlated (0.37) to the size of the P&L shock due to a common set of obligors defaulting on the asset and funding side. The correlation coefficient is increasing moving away from the tail of distribution, respectively 95$^{th}$ and 90$^{th}$ (0.42/0.67), since the set of defaulting counterparties is less homogeneous in the extreme tails, making funding and solvency shocks less correlated. This correlation is strengthened by bank runs across the whole distribution (0.54/0.45/0.68) and more materially in the far tail (VaR99) as by model dynamics described in section 3.5.1[37]. Contrary, the severity of funding shocks is less correlated (but still positively correlated) to total losses (post management actions) across the whole distribution, given that FS sales are triggered more by deleveraging needs than funding needs. Finally, the solvency contagion channel (SC) has negligible effects given the very limited exposure share among banks consistently with findings from Bardoscia et al. (2017).

[36] Conditional to the 99.5$^{th}$ percentile, our run-off rate increases up to 13% of the deposit base. For other examples of bank run numbers see Appendix F.

[37] We model the severity of funding withdrawals (bank runs) as an increasing function of banks' deteriorated solvency position.

5.3 Average Bank Probability of Default

As described in Section 3.7, we exploit the P&L distribution to assess whether banks' capital and liquidity ratios may fall below minimum regulatory requirements[38]. Thus, we compute the 1-year weighted average bank default probability pre (PD) and post-management actions (PD PMA) as reported in **Figure 3**. We find that the bank PD is historically floating around 0.43%, implying 1 bank default every ~ 230 years. Considering the potential impact from banks' management actions leads the bank default probability (PD PMA) to increase to 0.7% on average, or 1 bank default every ~ 143 years (Table 5)[39]. As would be expected, the PD was greater – and so the expected freqency of bank defaults higher – during the Covid pandemic when the economic outlook was adverse. Amplification mechanisms on a quarterly frequency account on average for 1/3 of contribution, although they show material variability over time. We do notice that the stability of the system has materially improved since 2015. PD PMA deacresed from 1.2% in 2015 to 0.3% in 2024. This finding is consistent with the improvement in banks' capital and liquidity ratios, respectively increasing by 2.5%, 2.8%, and 6.5% in terms of CET1, and TIER1 ratios, and cash ratio (Section 4 - Table 2), and also thanks to the reduction in CCaR99 estimates passing from £95 billion in 2015 to £79 billion in 2024.

**Figure 3:** 1-Year Weighted Average Bank Default Probability

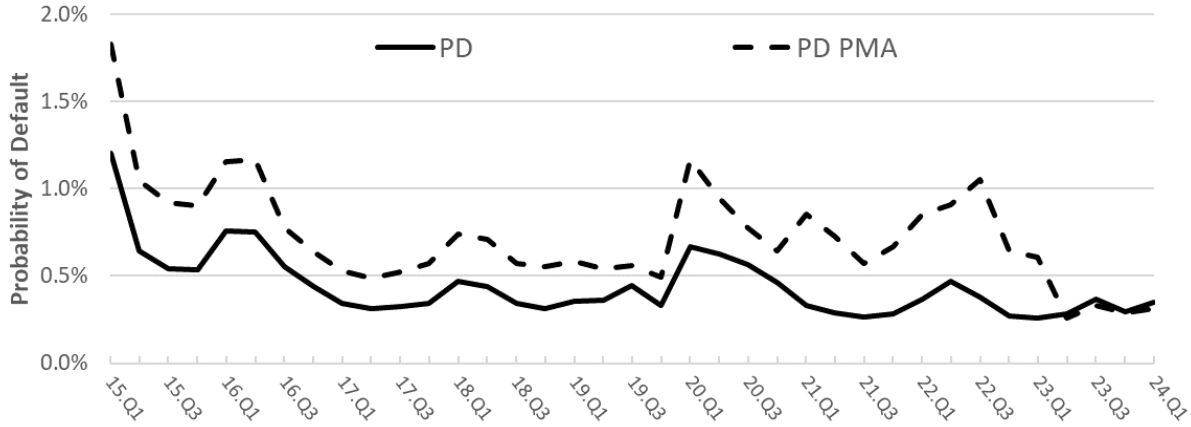


Note: PD refers to average bank default probability pre-management actions, while PD PMA refers to average bank PD post-management actions. Bank weights are kept constant across time for comparability purposes.

Notably, we find that management actions via fire sales deleveraging may also dampen the average bank default by 5 bps as shown in 2024. This negative effect is explained by the limited impact FS losses have in the tail of the loss distribution over the end of 2023 and 2024q1. Hence, in this recent period the deleveraging process seems to work effectively, reducing the numerator of the leverage ratio via asset sales faster than the reduction in the denominator

[38] We test the average bank PD sensitivity to changes in the CET1 default threshold (set at 7% throughout) in Appendix G, Table G5.
[39] The coefficient of variation is 42%.

(capital abse) from solvency shocks. This result is consistent with Shin and White (2020)'s findings based on the Federal Reserve's stress test, i.e. banks may improve their post-shock leverage ratio, as this depends on many factors such as asset size, initial leverage, and asset holdings.

Table 5: Bank Default Probability Decomposition by Channel
(Basis Points)

| | 2015 | 2016 | 2017 | 2018 | 2019 | 2020 | 2021 | 2022 | 2023 | 2024 | AVG |
|---|---|---|---|---|---|---|---|---|---|---|---|
| PD | 73 | 63 | 33 | 39 | 37 | 58 | 29 | 37 | 30 | 35 | 43 |
| FC | 1.9 | 1.8 | 0.6 | 0.3 | 0.7 | 1.4 | 0.9 | 0.3 | 0.5 | 0.7 | 0.9 |
| FS` | 42 | 29 | 19 | 25 | 16 | 29 | 41 | 49 | 7 | -5 | 25 |
| SC | 0.3 | 0.1 | 0.2 | 0.0 | 0.2 | 0.0 | 0.0 | 0.0 | 0.0 | 0.0 | 0.1 |
| PD PMA | 118 | 94 | 53 | 64 | 55 | 88 | 71 | 87 | 37 | 31 | 70 |
| DELTA | 45 | 31 | 20 | 25 | 17 | 30 | 41 | 49 | 7 | -4 | 26 |

Note: FC channel considers also defaults due to illiquidity. DELTA provides the difference between pre and post management actions (PD PMA - PD). Bank weights are kept constant across time for comparability purposes.

Furthermore, we find that bank runs and funding cost channels (FC) marginally exacerbate the average bank PD, by less than 2 bps. Nevertheless, the impact is conditional to a 90-days stress horizon and to the realized severity of the funding shocks. By stressing these two factors by increasing the stress horizon to 1-year and the funding shock size by 50%, we find that FC contribution to the PD PMA may increase by an additional 11 bps in 2015 and 1.5 bps in 2024 (Table 3G - Appendix G). This sensitivity test corroborates the result that the improvement in banks' liquidity positions (built up of cash reserves) have materially insured the UK banking system from material liquidity default events. In the end, the solvency contagion channel (SC) shows almost a negligible contribution. Digging into the determinants of banks' default, **Figure 4** reports the average bank default probability (unweighted) and decompose it by binding regulatory constraints. In this respect, we find that a bank is most commonly in default due to a simultaneous breach of both minimum CET1 ratio (7%) and leverage ratio (31) minimum requirements (PD_CET_LEV). This finding is in line with the complementary relationship between capital and leverage ratio found in Pfeifer et al. (2017): the leverage ratio to a certain extent mitigates the weaknesses of the capital ratio (model risk, and procyclicality), whereas the capital ratio reduces the risk of overweigh risky assets in the portfolio composition.

Next, we find that CET1 minimum requirements (PD_CET) are more binding in the first part of the sample than the leverage ratio (PD_LEV), whereas the opposite effect take place in the second part of the sample (post 2018). These results are in line with studies that focus on determinants of bank defaults via econometric techniques: big banks' defaults are affected more by insufficient capital buffers as found in Vazquez and Federico (2015). Furthermore, we find only a limited contribution from illiquidity-led default, as in line with Hong et al. (2014) findings. Moreover, this usually tends to be happening jointly with a breach of CET1

requirements in the first part of the sample consistently with the lower level of banks' liquidity reserves (CASH + HQLA) as presented in Table 4. Last, we compare the unweighted average and the weighted average (WPD) described previously. Overall, the two measures are very much positively correlated (0.8), with the unweighted average being roughly 40 bps higher compared to the weighted one[40].

**Figure 4**: Average Bank Default Probability (PMA) Decomposition by Default Thresholds

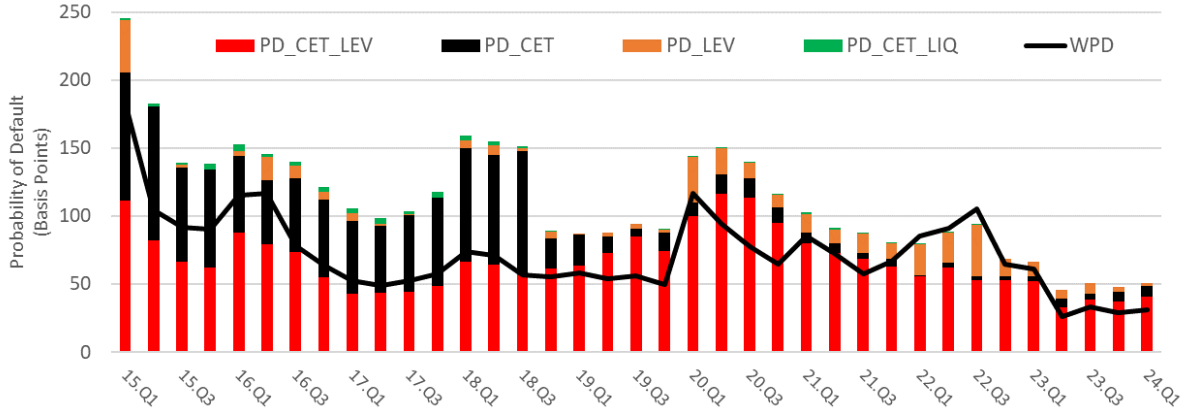


Note: WPD refers to the weighted average default probability.

In the end, to benchmark our estimates we provide a comparison with market-based probability of default retrieved from Eikon data source and based on Starmine Structural Credit Risk (SCR) model. Our approach differ from SCR model since the latter relies on a Merton model approach and on a firm's equity price to derive a 1-year default probability[41]. **Figure 5** compares the evolution of market-based PD with our model-based estimates and we show that PD estimates pre-management actions (the most comparable metric) tend to be very close to the market-based PD, respectively an average of 0.36% and 0.39% (Table 6)[42]. Nonetheless, a few material differences are visible during periods of high market volatility and uncertainty such as the Brexit referendum (2016) and the Pandemic period (2020-2021). Respectively during those periods, the market PD index tends to overshoot our PD estimates by 26 and 77 bps consistently with a higher sensitivity of market PD to banks' equity price volatility. Similarly, market PDs tend to re-adjust more materially once uncertainty unravels.

[40] Table G4 in Appendix G reports the detailed breakdown.

[41] Starmine Structural Credit Risk Model (SCR) evaluates the equity market's view of credit risk via StarMine's proprietary extension of the structural default prediction framework introduced by Robert Merton.

[42] We retrieve market-PD estimates for 5 banks out of 7 in our sample given stock market estimates are available only for the quoted firms. Consistently, we re-compute our weighted PD indexes matching the same sample of banks and by adjusting the vector of bank weights to sum-up to 1. We then weight the market PD by the same vector of bank weights to derive the weighted average market-based default probability for the banking sector.

**Figure 5**: Weighted Average Probability of Default Comparison with Market Estimates

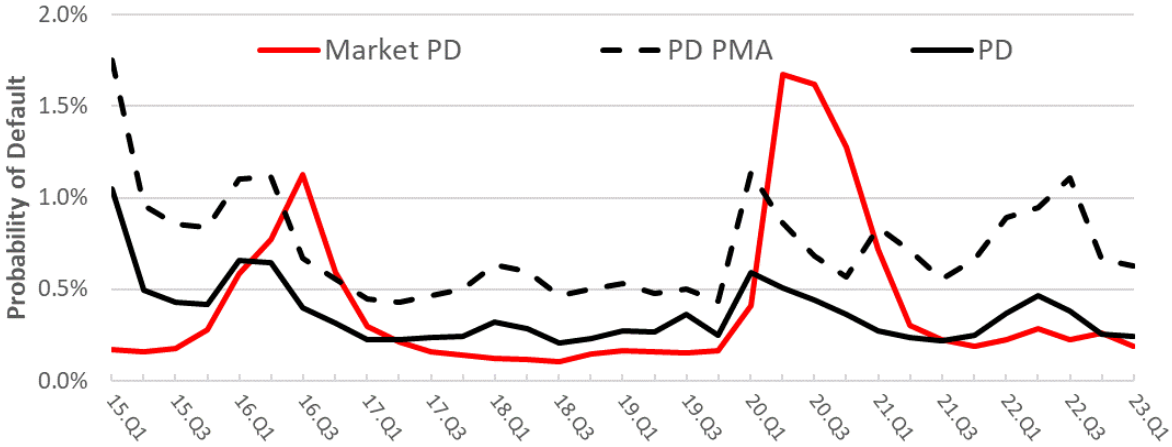


Note: Market PD refers to the weighted average bank default probability based on Starmine Structural Credit Risk Model (Merton model).

Overall, our PD index (pre-management actions) is a more stable indicator, capturing the increased level of downside risk without overshooting. Notably, our index is constructed exploiting a more complete set of information, capturing macro-financial developments via quarterly variation of banks' counterparty probability of default (capturing some degree of market impact), and more slow-moving input variables such as banks' balance sheet characteristics and banks' network of exposures. So, it is more anchored to banks' fundamentals and the structural features of the exposure network.

Clear evidence of this modelling contribution is shown during the Pandemic period. Our CCaR99 measure capturing tail risk developments materially increased by 25% relative to 2019, but its negative effect on average PD is compensated by a material improvement in banks' capital positions driven by the dividend restriction implemented by the Bank of England in April 2020 as response to the pandemic – average CET1 ratio increased from 14.2% to 15.8% (Table 2). This positive effect on banks' solvency position and system's financial stability works as an exacerbating factor in the Merton model since it contributes to further depress banks' equity prices relative to other sectors not subject to this policy measure. Our result is consistent with findings from Hardy (2021) who shows that bank equity prices fell with dividend restriction announcements, but credit default swap (CDS) spreads indicated that default risk either fell or was unaffected even in the face of the economic downturn. Furthermore, the market PD index tends also to overestimate our PD PMA index by 43 bps at the peak of the pandemic (2020). This result is consistent with findings from Majumder (2006), who highlights that equity prices are also governed by the irrational market movements, and so the price is the result of combined effect of firm-specific factor (fundamentals) and market-related factors, thereby leading the Merton model to overshoot relative to the firms'

fundamentals. Contrary, during periods of low volatility (uncertainty), our PD PMA index tends to be higher by 33 bps on average given it also considers a broader set of risks such as feedback and amplification mechanisms. This result is consistent with findings from Nagel and Purnanandam (2019), since standard structural models in which the asset volatility is assumed to be constant can understate banks' default risk in good times when asset values are high. Moreover, the different sensitivity to change in banks' solvency positions between the two models seem to be evident especially at the beginning of the sample, comparing 2015 estimates with 2017. In fact, the difference between our index and market index is the largest in 2015, respectively 40 bps (PD) and 90 bps (PD PMA), whereas in 2017 it is at its lowest, 3 bps and 26 bps, although market-based PD are in both years estimated to be at 0.2%. This material decrease in our PD index is consistent within our modelling framework given a material improvement in banks' average capital ratios, which increase by 2.2% (CET1 ratio) and 3% (TIER 1 ratio) as well as cash ratio by 3.3% between 2015 and 2017. Contrary, market-based PD underestimate banks' risks in 2015 given it is relatively a good period, whereas materially increase during the Brexit referendum (2016), and then gradually re-adjust to historical benign estimates in 2017.

Table 6: Bank Default Probability Decomposition by Channel
(Basis Points)

| | 2015 | 2016 | 2017 | 2018 | 2019 | 2020 | 2021 | 2022 | 2023 | AVG |
|---|---|---|---|---|---|---|---|---|---|---|
| PD MARKET | 20 | 77 | 20 | 12 | 16 | 125 | 36 | 25 | 19 | 39 |
| PD | 60 | 50 | 23 | 26 | 29 | 48 | 24 | 37 | 24 | 36 |
| PD PMA | 110 | 86 | 46 | 55 | 49 | 81 | 69 | 90 | 63 | 72 |
| DELTA PD PMA | 90 | 9 | 26 | 43 | 33 | -43 | 33 | 65 | 44 | 33 |
| DELTA PD | 40 | -26 | 3 | 14 | 13 | -77 | -12 | 12 | 5 | -3 |

Note: Market PD index reports the weighted average PD retrieved from market data based on Starmine Structural Credit Risk Model (SCR). DELTA PD (PMA) reports the difference between PD (PMA) and Market PD.
Source: LSEG Eikon Data source and authors' calculations.

Finally, we provide a comparison of our PD indicator with actual data on financial institutions' default rates. Although we acknowledge that these two indicators are not one-to-one comparable since the latter are affected also from other mitigating factors such as policy interventions which are not included in our estimates, the Standard & Poor (S&P 2024) global financial institutions' 1-year default rate during the pandemic period (2020-21) reached 0.5% (versus 0.8% we estimate), whereas in 2015-16 it was close to 1% (versus 1.1%). Moreover, the US commercial bank default rate reported by the FDIC (Figure G2 Appendix) between 2020-21 is close to 0.3%, with an average of 0.25% over the last 10 years. Overall, we can argue, keeping in mind the underlying different sample of firms, that our model-based PD estimates tend to be higher relative to actual default rates by roughly 20 bps on average. All in all, although some differences in the estimated PD levels, which can be reconciled to some

extent and motivated, the microstructural methodology seems to perform well, re-assuring about its sound calibration and strengthening the set of results up to here presented. This is a key outcome in relation to the existing microstructural balance sheet network literature since for the first time such type of models can be back-tested against market-based approaches. This is an important step since the value added of our methodology resides in its microstructural derivation, that is, modelling each part of the system with endogenous dynamics. Hence the methodology can be tested as a policy laboratory in which a prudential policy assessment (micro and macro) can be carried out via counterfactual policy exercises as pointed out by Aikman et al. (2024). This application will be presented in the next section.

## 6 Macroprudential Policy Assessment

Relying on the methodology as a policy laboratory, we can vary a part of the system to test how the output variables change conditional to this exogenous shock. Specifically, a change to the regulatory environment can be interpreted as an exogenous policy shock and in turn assess its impact on a bank basis or at the level of the system. We have limited the assessment to the system perspective (macroprudential) given the confidentiality of the data which does not allow us to showcase bank-specific results.

*Policy Target and Tools*

As first step, we can use the weighted average bank PD as the policy maker's key quantitative indicator to track financial stability risk in the banking system. In a similar vein to how monetary policy rules are used in research in that domain, for the purposes of experimentation we can define a policy target or risk tolerance of the regulator, which can be calibrated as a strict target or confidence band. Looking at the estimated PD indicators (Figure 3) and excluding the Pandemic period which represents stress conditions (2020-21) and the pre-Brexit period (2015-16) in which capital ratios were well below current levels, we can suppose for the sake of experimentation that the regulator's risk tolerance in *normal times* may float around 0.5% with some tolerance for values on either side, and in *bad times* may rise above 1% as seen during the pandemic period[43].

Next, given the PD indicators are a direct function of banks' capital and liquidity ratios - as described in Section 3 and in Appendix C - we can identify them as intermediate targets used

[43] The exclusion of these two periods is motivated with the following reasons. The initial period (2015-16) is not representative given that the first three BoE stress test exercises revealed some capital inadequacies and sizeable drawdowns in capital ratios which culminated with recommendations to banks to strengthen their capital positions. Similarly, the Pandemic period (2020-21) is not representative of normal risk preferences since in response to this extreme shock, the BoE has implemented a dividend restriction crisis tool.

to steer the banking system's average PD. These intermediate targets are endogenously modelled and hence can be shocked to assess via counterfactual exercises the impact on the average bank PD. From a regulatory perspective, capital and liquidity buffer requirements such as the Countercyclical Capital Buffer (CCyB) or Liquidity Coverage Ratio (LCR) are used as policy tools by regulators to affect the intermediate targets, dynamically as in the former case or statically as in the latter. Other tools such dividend restrictions can be introduced to offset sudden shocks (boosting capital via the retained earnings channel) more promptly than conventional tools like the CCyB which has an implementation lag of one year between the announcement date and its mandatory compliance. Furthermore, during a period of high uncertainty and capital market disruption, rising capital (bank capital channel) by issuing new shares may become too costly. Hence, banks may instead reduce lending to meet regulatory capital requirements thereby producing real negative effects on consumption and investment (Van den Heuvel, 2002).

Accordingly, we perform two exploratory counterfactual policy exercises showcasing respectively: i) the role and impact of a dividend restrictions; and ii) a macroprudential exercise for assessing the calibration of banks' capital requirement.

### 6.1 Dividend Restrictions

This is a tool which has been widely used by central banks (BOE, ECB) during the exceptional circumstances triggered by the 2020-21 Pandemic (Hardy, 2021; Marsh, 2023). It had a material impact on banks' capital base measured as CET1 and TIER1 capital increase over this period, respectively passing from 14.2% and 17.1% in Q1-2020 to 15.8% and 18.9% in 2021. Although it is evident that banks' solvency position has materially improved given the improvement in the intermediate policy targets, it is not straightforward for a policy maker to quantify the impact on the overall banking system's stability - ultimate policy target. In theory, a policy maker may also decide to constrain dividend payouts to be a share of total expected payouts and this decision/assessment requires estimating the impact on the ultimate policy target and a well-defined risk tolerance. In this respect, our framework provides those bearings and via counterfactual policy exercise can shed light on this trade-off. Specifically, we intend to measure the impact from a mechanical reduction of banks' capital base (what if scenario), and the endogenous F&A effects that banks' management action may provoke[44]. Hence, we test a what if scenario in which no dividend restrictions are implemented, thereby keeping the

[44] The methodology models endogenous effects stemming from a reduced distant to solvency distress thresholds, which affect banks' management actions and in turn the severity of amplification mechanisms relative to the realized outcome.

level of banks' capital base (CET1 and TIER1) equal to 2020q1 till end of 2021q4. Thus, we quantify by how much this tool has contributed to reduce the weighted average bank default probability assuming all else being equal[45].

**Figure 6** reports the weighted average bank default probability under this counterfactual scenario without (PD NO DR) and with banks' management actions (PD PMA NO DR). We find that the average bank default probability without the implementation of dividend restrictions would have been on average higher by roughly 32 bps over 2020 and 2021. This finding is in line with literature on effects of dividend restrictions that focused on Covid-19 period in particular Dautović et al. (2023) and Acosta-Smith et al. (2023).

**Figure 6**: Impact of Dividend Restrictions on Banks' Default Probability

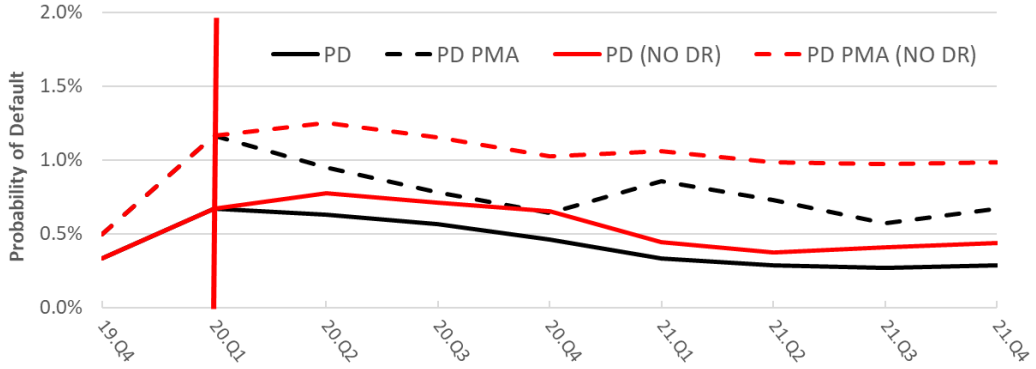


Note: NO DR refers to the counterfactual simulation as if no Dividend Restrictions were implemented.

Specifically, as reported in Table 7, we quantify that the mechanical impact from a lower capital base contributes to increase the average bank default probability (pre management actions) by 14 bps (DELTA PD). On top of this, the change in the capital base makes also banks to be more reactive to shocks, requiring them to deleverage more and experience more severe funding shocks given the distress thresholds are more likely to become binding. In this respect, we estimate that these endogenous effects contribute to increase the average bank PD post management actions by an additional 18 bps, on average. Overall, we can state that the dividend restrictions crisis tool implemented by the regulator in 2020q1 was extremely effective in keeping banking stability under control and close to the hypothetical risk tolerance level we have assumed for the regulator during this exceptional stress period. Benefits were

[45] We acknowledge that we cannot exclude the positive endogenous effects that the DR had on mitigating risks in the real economy since it helped to sustain bank lending to corporates (Hardy, 2021). Hence, we can consider our estimates to be conservative, the positive effects would be even greater. This is also the reason why it was implemented given that rising capital during a downturn can be costly and also unfeasible given markets and investors may be less willing to provide equity injections.

not limited to the microprudential sphere of individual banks' PD, but also played an effective macroprudential role by curbing potential endogenous spillovers[46].

Table 7: Dividend Restrictions and Bank Default Probability (Basis Points)

| | 20.Q2 | 20.Q3 | 20.Q4 | 21.Q1 | 21.Q2 | 21.Q3 | 21.Q4 | AVG |
|---|---|---|---|---|---|---|---|---|
| PD DR | 78 | 71 | 65 | 44 | 38 | 41 | 44 | 54 |
| PD | 63 | 57 | 46 | 33 | 29 | 27 | 29 | 40 |
| DELTA PD | 15 | 14 | 19 | 11 | 9 | 14 | 15 | 14 |
| PD PMA DR | 47 | 45 | 37 | 62 | 61 | 57 | 55 | 52 |
| PD PMA | 32 | 21 | 18 | 53 | 44 | 31 | 38 | 34 |
| DELTA PD PMA | 15 | 23 | 19 | 9 | 17 | 26 | 17 | 18 |
| DELTA PD TOT | 30 | 38 | 38 | 20 | 26 | 40 | 32 | 32 |

Note: DELTA PD and DELTA PD PMA refer to the difference between baseline estimates (Table 5) and counterfactuals based on no dividend restrictions (DR).

## 6.2 Macroprudential Stress Testing and Capital Calibration

Lastly, we showcase how the methodology can be used as a macroprudential stress testing capital calibration tool. Up to here, we have tested the methodology conditional to historical central-case macro-financial conditions realized over the period 2015-2024. Now we perform a stress testing exercise in which macro-financial conditions materially deteriorates over 1-year horizon in line with the Bank of England 2024 adverse scenario (BOE 2024). This stress scenario is calibrated to approximate the 99$^{th}$ percentile of the historical distribution of macro-financial conditions jointly with rising interest rates thereby resembling a severe event. Consistently, via satellite credit risk models we translate this change in macro-financial conditions into a change in banks' counterparty PDs - key inputs of the methodology[47] - keeping all else equal to 2024q1 snapshot date in terms of banks' portfolio allocation and balance sheet positions. Next, we re-estimate the model and assess the change in the average bank default probability over 1-year horizon (up to 2025q1).

**Figure 8** shows that the bank average PD would increase from 31 bps in 2024q1 to 2.5% in 2025q1 (after 1 year) driven by core PD ST estimates stemming from credit and market risk losses (without management actions - PMA). Nonetheless, amplifying effects from banks' management actions (proxy by the gap between PD ST and PD PMA ST) become material (33 bps increase or 15%) especially at the peak of the stress in Q1-2025[48]. Specifically, the funding cost channel and the illiquidity channel become more relevant than baseline estimates in Q1-

[46] These estimates are conservative since they don't capture the lower level of lending and in turn the higher economic risk the no policy scenario would have entailed.

[47] For a better interpretability of the results, we keep exposure-specific loss-given-default parameters (LGD) unchanged relative to Q1-2024 (without stress). Moreover, we retain the same correlation structure used for the entire analysis. Both sets of parameters according to the credit risk literature are supposed to increase during a stress period. Hence, our estimates may be judged as non-conservative.

[48] We estimate that CaR99 total losses reach £160 billion in Q1-2025 (£34 bn from PMA) relative to £79 billion estimated pre-stress in Q1-2024 (£19 billion from PMA).

2024, contributing to the increase in the bank average PD PMA ST by 26 bps. Furthermore, we estimate that at the peak of the stress (Q1-2025) the expected liquidity outflows for VaR99 (LaR99) would reach £850 billion, in comparison to £185 billion in Q1-2024. This estimate is consistent with the amount of liquidity outflows (£875 billion) assumed in the LCR calibration for the same set of banks as of Q1-2024. Contrary, the fire-sales channel seems to play a smaller role compared to liquidity-solvency spillovers thanks to the low-risk composition (HQLA ~ 44% of securities) of banks' security portfolio as of 2024q1 (as shown in Section 4)[49].

In this respect, the bank average PD may increase under the stress scenario well above the regulator's risk tolerance in normal times and much beyond the levels experienced during the pandemic period. During such stress conditions, the regulator may be willing to accept temporarily a higher-level of systemic risk in the banking system, depending on its risk tolerance, in order to support continued lending to creditworthy households and businesses. Or the policymaker may seek to take action to reduce the probability of default, for example by introducing dividend restrictions. We can assess what would be the impact of an associated homogeneous increase in banks' core capital on the average bank default probability over the stress horizon.

**Figure 8**: Weighted Average Probability of Default - Adverse Scenario

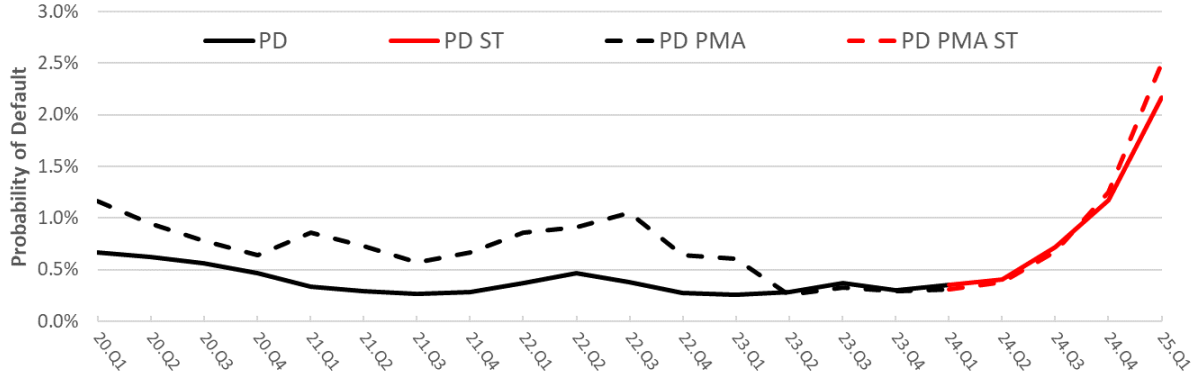


Note: PD ST and PD PMA ST refer to the weighted average bank PD estimates conditional to the adverse scenario.

**Figure 9** shows that a higher capital base (CET1 and TIER1 capital) by 50, 100, 150 or 200 basis points of RWAs (increasing the distant to default) may reduce the average bank PD respectively from 2.5% to 1.9%, 1.5%, 1.3% and 1% at the peak of the stress. Hence, dividend restrictions of similar size to the one implemented during the pandemic (i.e ~ 200 bps increase in the capital base) would be effective in bringing the average bank PD close to 1%. The timing

[49] Interestingly, the model dynamics shows that FS channel would both increase the average bank default probability at the peak of the stress (Q1-2025) by 15 bps in the first round and reduce it by 8 bps in the second round, resulting in a net positive effect of 7 bps. This net impact would have been larger if we had used a more equity-based risky portfolio allocation than the current one.

of a DR implementation and the severity of the stress do affect the size of banks' potential retained earnings making its precise calibration a difficult task. Notably, we find that this impact is non-linear with decreasing marginal returns from increasing banks' capital base beyond 50 bps. In fact, a capital injection of 50 bps, passing from 0 to 50 bps, would decrease the average bank PD by 24%, and further (additional 50 bps increase) passing from 50 bps to 100 bps by 19%, and by 18% when we move from 100 bps to 150 bps (and similarly from 150 bps to 200 bps). This uplift in the capital base can be also achieved through a combination of policies aiming to strengthen banks' capital positions in advance of the stress (Van Oordt, 2023). For instance, the regulator may opt to increase banks' capital buffers by 50 bps so as to push up banks' capital over time. This higher capital base would have a limited positive effect on reducing banks' PDs under normal conditions as of 2024q1 (1 to 5 bps), although it may be optimal when severe stress conditions materialize.

**Figure 9**: Weighted Average Probability of Default - Stress Scenario and Capital Calibration

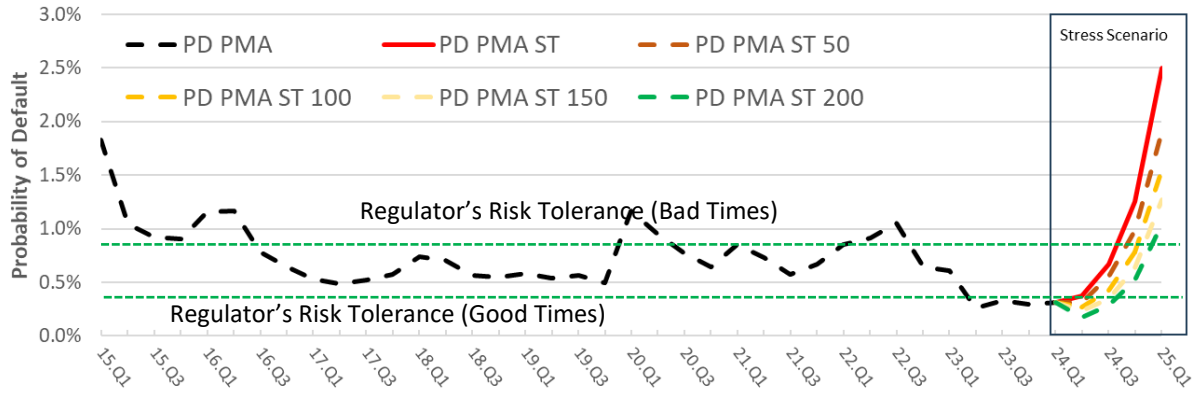


Note: PD PMA ST refer to the weighted average bank PD estimates conditional to the adverse scenario. Moreover, the PD PMA ST 50/100/150/200 refer to the weighted average bank PD estimates under the adverse scenario adjusted by a capital increase of X basis points. Green dotted bands proxy regulator's risk tolerance level, respectively in good and bad times.

To avoid acting procyclically a countercyclical policymaker should set capital in normal times so as the PD would remain within its risk tolerance even in stress scenarios. However, it faces uncertainty over how severe a stress scenario may be, and if it sets capital too high in normal times, it may restrain the banking system from optimally lending to the real economy and so potentially tightening the financial and the economic cycle in undesirable way, leading to the so called "stability of the graveyard" in the absence of shocks. Hence, capital buffer calibration policies and dividend restriction measures are indeed good complementary tools, the former providing ex ante resilience to a scenario up to a particular severity and the latter leaving space to the regulator to affect its policy target (AVG PD) given the changing macro-financial conditions when needed, thereby avoiding the negative effects of a too tight capital policy during normal times.

## Concluding Remarks

This paper develops a microstructural methodology modelling jointly solvency and liquidity risks and their interactions in the banking system to provide a macroprudential assessment of systemic risk in the banking system. Concerns have been raised over the lack of regulatory stress tests that capture liquidity risk and its spillovers to the solvency dimension given the period of banking distress in the US in 2013. In this paper, we test and back-test our methodology providing a risk assessment in terms of bank default probability and its drivers over a 10-year period and on a quarterly basis for the UK banking system.

Against this background, we show that funding risk correlates materially on a portfolio level with solvency risk given the set of banks' borrowers and funding sources do overlap, thereby transmitting shocks on both sides of the balance sheet simultaneously. Furthermore, when we introduce banks' behavioural responses and potential market reactions, this relationship further tightens, creating the conditions for potentially harmful reinforcing amplification mechanisms.

Next, we find that in recent years the UK banking system has had enough capital and liquidity to withstand and absorb potential severe shocks, thereby avoiding severe feedback-loops between these two dimensions. We show that this finding holds even under stress conditions experienced during the covid pandemic as well as under a hypothetical GFC-type stress scenario, although in the latter case the impact increases especially due to liquidity-driven solvency spillovers. In this respect, we highlight that mitigating effects stem from the material build-up in banks' cash reserves and improvement in banks' capital ratios between 2015 and 2024, the period of analysis. These two mitigating factors combined with banks' de-risking in terms of portfolio composition have reduced the severity of potential credit and market risk losses in the tail as well as feedback and amplification mechanisms.

Finally, we showcase the positive impact the introduction of dividend restrictions had at keeping financial stability risks under control when macro-financial conditions deteriorated sharply with the unfolding of the pandemic. This tool has indeed been proved to be an effective crisis tool with complementary benefits to other more conventional measures such as the countercyclical capital buffer. Overall, the methodology can be used as a policy laboratory to monitor the stability of the banking system in real time, assess the effectiveness of policy changes as well as their calibration according to a measurable policy target - average bank default probability - and conditional to a regulator's risk tolerance.

## References

Acharya, V.V., and O. Merrouche (2012), "Precautionary Hoarding of Liquidity and Interbank Markets: Evidence from the Subprime Crisis", *Review of Finance*, 17(1):107-160.

Acharya V.V., Engle R.F., and D. Pierret (2014), "Testing Macroprudential Stress Tests: The Risk of Regulatory Risk Weights", *Journal of Monetary Economics*, 65:36-53

Acharya V.V. and Raghuram R., (2022), "Liquidity, Liquidity Everywhere, Not a Drop to Use: Why Flooding Banks with Central Bank Reserves May Not Expand Liquidity", NBER WP No. 29680

Acharya V.V. and D. R. Skeie (2011), "A Model of Liquidity Hoarding and Term Premia in Inter-Bank Markets", *Journal of Monetary Economics* , 58:436-447

Acosta-Smith J., J. Barunik, E, Gerba, and P. Katsoulis (2023), "Moderation or indulgence? Effects of bank distribution restrictions during stress", Bank of England WP No. 1053

Aikman D., D. Beale, A. Brinley-Codd, G. Covi, A-C. Huser, and C. Lepore (2023), "Macroprudential Stress Test Models: A Survey", Bank of England WP No. 1037.

Albertazzi U. and L. Gambacorta (2009), "Bank Profitability and the Business Cycle", *Journal of Financial Stability*, 5(4):393-409

Aldasoro I., and E. Faia (2016), "Systemic loops and liquidity regulation, *Journal of Financial Stability*, 27:1-16

Allen, F., Covi, G., Gu, X., Kowalewski, O., Montagna, M. (2020). The interbank market puzzle, Bank of England WP No. 862

Allen, F., and D. Gale (2000), "Financial contagion", *Journal of Political Economy*, 108(1)1-33

Arinaminpathy N., S. Kapadia, and R. M. May (2012), "Size and complexity in model financial systems," *Proceedings of the National Academy of Sciences of the United States of America*, 109(45):18338-18343

Anderson R., Danielsson J., Baba C., Das U.S., Kang H., M. Segoviano (2018), "Macroprudential Stress Tests and Policies: Searching for Robust and Implementable Frameworks", International Monetary Found WP No. 18/197

Annaert J., M. De Ceuster, P. Van Roy and C. Vespro (2013), "What determines Euro area bank CDS spreads?" *Journal of International Money and Finance* 32: 444–461

Armour J., D. Awrey, P. Davies, L. Enriques, J.N. Gordon, C. Mayer, and J. Payne (2016), "Principles of Financial Regulation", ECGI in Law WP No. 277/2014.

Arnould, G., G. Avignone, C. Pancaro, D. Zochowski (2022), "Bank funding costs and solvency", *The European Journal of Finance*, 28(10): 931-963.

Aymanns C., J.D. Farmer, A.M. Kleinnijenhius, T.Wetzer (2018), *Models of financial stability and their application in stress tests*, Hanbook of Computational Economics, 4, pp. 329-391.

Babihuga R. and M. Spaltro (2014), "Bank Funding Costs for International Banks", International Monetary Found, WP No. 14/71

Banks of England (2017), "UK leverage ratio: treatment of claims on central banks", Policy Statement PS21/17

Bardoscia M., P. Barucca, A. Brinley-Codd and J. Hill (2017), "The decline of solvency contagion risk," Bank of England WP. No. 662

BCBS (2013). Liquidity stress testing: a survey of theory, empirics and current industry and supervisory practices, Basel Committee on Banking Supervision, working paper, No. 24.

BCBS (2015). Making supervisory stress tests more macroprudential: Considering liquidity and solvency interactions and systemic risk, Working Paper No 29, Basel Committee on Banking Supervision.

Benbouzid N., A. Kumar, K. Mallick, R. Sousa (2022), "Bank credit risk and macro-prudential policies: Role of counter-cyclical capital buffer", *Journal of Financial Stability* 63(2)

Benzoni L., Collin-Dufresne P., Goldstein R.S., and J. Helwege (2015), "Modelling credit contagion via the updating of fragile beliefs", *Review of Financial Studies* 28, 1960-2008

Bechara B., A. Bernales, C. Canon, N. Garrido (2024), "Aggregate Risk and Lending Decisions in the Interbank Market", *Journal of Money credit and Banking*, 2024

Berrospide, J. (2021), "Liquidity Hoarding and the Financial Crisis: An Empirical Evaluation", *Quarterly Journal of Finance*, 11(4):1-35

Bindseil, U. (2013). Central bank collateral, asset fire sales, regulation and liquidity, European Central Bank WP No. 1610

Bindseil U. and R. Senner (2024), "Destabilisation of bank deposits across destinations: assessment and policy implications", European Central Bank WP No. 2887

Blicke, K., Brunnermeier, M., Luck, S. (2024), Who Can Tell Which Banks Will Fail?", The Review of Financial Studies 00:1-47.

BOE (2024), "Stress testing the UK banking system: scenarios for the 2024 desk-based stress test", Available at Link.

BOE (2022). Jon Cunliffe: Learning from the dash for cash – findings and next steps for margining practices. Available at: Link.

Bolt W., L. De Haan, M. Hoeberichts, M.R.C. Van Oordt, J. Swank (2012), "Bank profitability during recessions", *Journal of Banking and Finance*, 36(9):2552-2564

Bonfim D. and C. Santos, (2004), "Determinants of Banks's Financing Costs in the Bond Market", Banco de Portugal, Financial Stability Report.

Caccioli, F., Ferrara G., A. Ramadiah (2024), "Modelling fire sale contagion among banks and non-banks", *Journal of Financial Stability* 71

Caccioli, F., Farmer, J. D., Foti, N., and Rockmore, D. (2015). Overlapping portfolios, contagion, and financial stability. *Journal of Economic Dynamics and Control*, 51:50–63.

Caccioli, F., Shrestha, M., Moore, C., and Farmer, J. D. (2014). Stability analysis of financial contagion due to overlapping portfolios. Journal of Banking & Finance, 46:233–245.

Cetorelli, N. and L. Goldberg (2016), "Organizational complexity and balance sheet management in global banks", National Bureau of Economic Research WP No. 22169

Coen J., C. Lepore, and E. Schaanning, (2019), "Taking regulation seriously: fire sales under solvency and liquidity constraints", Bank of England WP No. 793

Cont, R., Kotlicki, A., and L. Valderrama (2020), "Liquidity at risk: Joint stress test of solvency and liquidity", *Journal of Banking & Finance* 118.

Cont R. and E. Schaanning (2019), "Monitoring indirect contagion", *Journal of Banking & Finance*, 104(c): 85-102

Cont, R. and Schaanning, E. (2017). Fire sales, indirect contagion and systemic stress testing. Norges Bank WP No. 2/2017

Coulier Cyril and V. Scalone (2021), "Risk-to-Buffer: Setting Cyclical and Structural Capital Buffers through Banks Stress Tests", Banque de France WP 830

Covi G. and A-C. Huser (2024), "Measuring Capital at Risk with financial contagion: two-sector model with banks and insurers", Bank of England WP No. 1081

Covi, G., Brookes, J., and Raja, C. (2022). Measuring capital at risk in the UK banking sector. Bank of England Working Paper No. 983

Covi G., M. Gorpe, and C. Kok (2021), "CoMap: Mapping Contagion in the Euro Area Banking Sector", *Journal of Financial Stability* 53

Covi, G., M. Gorpe, and C. Kok (2019), "An Adaptive Contagion Mapping Methodology", SSRN Working Paper

Counsel G. (1994), Banesto customers in rush to withdraw deposits. Available at Link.

Davidovic S., A. Kothiyal, M. Galesic, K. Katsikopoulos, and N. Arinaminpathy (2019), "Liquidity Hoarding in Financial Networks: The Role of Structural Uncertainty", *Complexity* 2019:1-16.

Dautović E., L. Gambacorta, A. Reghezza (2023), "Supervisory Policy Stimulus: Evidence from the Euro Area Dividend Recommendation", BIS WP No. 1085

De Fiore, F., Hoerova, M., and H. Uhlig (2017), "The Macroeconomic Impact of Money Market Disruptions", European Central Bank Working Paper

Dehmej, S., Gambacorta, L. (2019), "Macroprudential Policy in a Monetary Union", *Comparative Economic Studies*, 61:195-212.

Dent, H., Hoke, S.H., and A. Panagiotopoulos (2021), "Solvency and wholesale funding cost interactions at UK banks", *Journal of Financial Stability*, 52:100799.

Di Filippo, M., Ranaldo, A., Wrampelmeyer, J. (2020), "Unsecured and Secured Funding", *Journal of Money, Credit and Banking*, 54 (2-3): 651-662.

Diamond, D.W., and R.G. Rajan (2005), "Liquidity Shortages and Banking Crises", *The Journal of Finance*, 60(2):615-647.

Duarte F. and T.M. Eisenback, (2021), "Fire-Sale Spillovers and Systemic Risk", *The Journal of Finance*, 76(3):1251-1294

Duncan E., A. Horvath, D. Iercosan, B. Loudis, A. Maddrey, F. Martinez, T. Mooney, B. Ranish, K. Wang, M. Warusawitharana, and C. Wix (2022), "COVID-19 as a stress test: assessing the bank regulatory framework", *Journal of Financial Stability* 61

EBA (2022). ECB assesses that Sberbank Europe AG and its subsidiaries in Croatia and Slovenia are failing or likely to fail. Available at: Link.

EBA (2022b). ECB Annual Report on supervisory activities. European Banking Authority.

Eisenberg, L. and T. H. Noe (2001), "Systemic risk in financial systems", *Management Science*, 47(2):236-249

Elsinger H., A. Lehar, and M. Summer (2006), "Risk Assessment for Banking Systems", *Management Science* 52(9):1301-14

Esparcia, C., Escribando, A., and F. Jareño (2023), "Did crypto market chaos unleash Silvergate's bankruptcy? Investigating the high-frequency volatility and connectedness behind the collapse", *Journal of International Financial Markets, Institutions and Money* 89

Farmer J.D., A.M. Kleinnijenhius, P. Nahai-Williamson, and T. Wetzer (2020), "Foundations of system-wide financial stress testing with heterogeneous institutions", Bank of England WP No. 861

FDIC (2009). Information for IndyMac Bank, F.S.B., and IndyMac Federal Bank, F.S.B., Pasadena, CA. Available at: Link.

FED (2023a). Re: Review of the Federal Reserve's Supervision and Regulation of Silicon Valley Bank.

FED (2023b). Understanding the Speed and Size of Bank Runs in Historical Comparison, by Jonathan Rose. Available at Link.

Fukker, G., Kaijser, M., Mingarelli, L., and M. Sydow (2022), "Contagion from market price impact: a price-at-risk perspective", European Central Bank WP No. 2692

Gai P. and S. Kapadia (2010), "Contagion in financial networks", *Proceedings of the Royal Society A: Mathematical, Physical and Engineering Sciences*, 466(2120):2401-2423

Gale D. and T. Yorulmazer (2013), "Liquidity hoarding", *Theoretical Economics* 8:291-324

Glasserman, P. (2004). "Tail approximations for portfolio credit risk", *Journal of Derivatives*, 12(2):24–42

Glasserman P. (2005), "Measuring marginal risk contributions in credit portfolios", *Journal of Computational Finance* 9:1-41

Glasserman P. and H.P. Young (2016), "Contagion in financial networks", *Journal of Economic Literature*, 54(3):779–831

Gorton G. (2017), "The history of economics of safe assets", *Annual Review of Economics*, 9:547-586

Greenlaw D., A. Kashyap, K. Schoenholtz and H. Shin (2012), "Stressed out: Macroprudential principles for stress testing", The University of Chicago, Booth School of Business WP 71

Greenwood R., A. Landier, and D. Thesmar (2015), "Vulnerable banks", *Journal of Financial Economics*, 115(3): 471-485.

Guisio L., Sapienza P., L. Zingales (2018), "Time varying risk aversion", *Journal of Financial Economics* 128(3):403-421

Hałaj G. (2018), "System-wide implications of funding risk", *Physica A* 503(2018):1151-1181

Hałaj G. (2020), "Resilience of Canadian banks to funding liquidity shocks", *Latin American Journal of Central Banking*, 1:100002

Hałaj, G., and S. Priazhkina (2021), "Stressed but not Helpless: Strategic Behaviour of Banks Under Adverse Market Conditions", Bank of Canada No. 2021-35

Hardy B. (2021), "Covid-19 bank dividend payout restrictions: effects and trade-offs", BIS Bulletin 38, retrieved from: https://www.bis.org/publ/bisbull38.pdf

Hasan I., L. Liu, G. Zhang (2016), "The Determinants of Global Bank Credit-Default-Swap Spreads", *Journal of Financial Services Research*, 50: 275-309.

Heider F., M. Hoerova and C. Holthausen (2009), "Liquidity hoarding and interbank market spreads: The role of counterparty risk", *Journal of Financial Economics* 118(2):336-354

Hoerova, M., and C. Monnet (2016), "Money Market Discipline and Central Bank Lending", European Central Bank WP, presented at the workshop on the "Post-crisis design of the operational framework", European Central Bank, October 2011.

Hong, H., J.-Z Huang, and D. Wu (2014), "The information content of Basel III liquidity risk measures", *Journal of Financial Stability* 15

Iyer R., and JL. Peydró (2011), "Interbank Contagion at Work: Evidence from a Natural Experiment", *The Review of Financial Studies*, 24(4):1337-1377

IMF (2013). Republic of Latvia: Ex Post Evaluation of Exceptional Access Under the 2008 Stand-By Arrangement; Public Information Notice on the Executive Board Discussion; and Statement by the Executive Director for the Republic of Latvia, IMF country report No. 13/30. Available at Link.

Korsgaard S. (2021), "Incorporating funding costs in top-down stress tests", *Journal of Financial Stability*, 52:100798.

Jiang H., D. Li, and A. Wang (2021), "Dynamic Liquidity Management by Corporate Bond Mutual Funds", *Journal of Financial and Quantitative Analysis* 56(5):1622-1652

LSEG, London Stock Exchange Group Data & Analytics, "StarMine Structural Credit Risk Model", retrieved from Link.

Lo, AW (2017). *Adaptive markets: Financial evolution at the speed of thought*, Princeton University Press.

Marsh W. B. (2023), "Supervisory stringency, payout restrictions, and bank equity prices" *Journal of Financial Stability* 154

Montagna, M., Covi, G., Torri, G. (2020), "On the origin of systemic risk". Bank of England WP No. 906.

Majumder D. (2006), "Inefficient markets and credit risk modelling: Why Merton's model failed", *Journal of Policy Modelling* 28(3):307-318

Matyunina A. and S. Ongega (2022), "Bank capital buffer releases, public guarantee programs, and dividend bans in COVID-19 Europe: an appraisal", *European Journal of Law and Economics* 54:127-152

McCandless, G., Gabrielli, M.F., M.J. Rouillet (2003), "Determining the Causes of Bank Runs in Argentina During the Crisis of 2001", *Revista de Analisis Economico* 18(1)

Nagel, S. (2016). "The liquidity premium of near money assets", *The Quarterly Journal of Economics*, 131:1927-1971

Nagel S. and A. Purnanandam (2019), "Bank Risk Dynamics and Distance to Default", NBER WP No. 25807

Pfeifer L, L. Holub, Z. Pikhart, and M. Hodula (2017). "Leverage Ratio and its Impact on the Resilience of the Banking Sector and Efficiency of Macroprudential Policy." *Czech Journal of Economics and Finance* 67 (4): 277-299

Pierret, D. (2015). "Systemic Risk and the Solvency-Liquidity Nexus of Banks", *International Journal of Central Banking*, 11(3):193-227.

Piquard, T., and D. Salakhova (2019), "Secured and Unsecured Interbank Markets: Monetary Policy, Substitution and the Cost of Collateral", Banque de France WP No. 730

Pruyt, E., and C. Hamarat (2010), "The Concerted Run on the DSB Bank: An Exploratory System Dynamics Approach", Proceedings of the 18th International Conference of the System Dynamics Society, Seoul, Korea. Available at Link.

Puhr, C. and Schmitz, S.W. (2014), "A view from the top – the interaction between solvency and liquidity stress", Journal of Risk Management in Financial Institutions, 7(1):38-51

Ramadiah A., Fricke D., and F. Caccioli (2022), "Backtesting macroprudential stress test", *Journal of Economic Dynamics and Control,* 137

Rochet, J-C., and X. Vives (2004), "Coordination Failures and the Lender of Last Resort: Was Bagehot Right After All?", *Journal of the European Economic Association* 2(6):1116-1147.

Schaanning, E. F. (2016). Fire sales and systemic risk in financial networks. PhD thesis, Imperial College London

Shleifer A. and R. Vishny (2011), "Fire sales in finance and macroeconomics", *Journal of Economic Perspectives*, 25(1):29–48

Schmieder, C., Hesse, H., Neudorfer, B., Puhr, C., and S.W. Schmitz (2012), „Next generation system-wide liquidity stress testing", International Monetary Fund WP No. 12/3

Schmeider, C., Hesse, H., Neudorfer, B., Puhr, C., S.W. Schmitz (2011), "Next Generation System-Wide Liquidity Stress Testing", International Monetary Fund WP No.12/3

Schmitz, S. W., Sigmund, M., and L. Valderrama (2019), "The interaction between bank solvency and funding costs: A crucial effect in stress tests", *Economic Notes* 48:12130.

Schmitz, S.W., Sigumund, M., Valderrama, L. (2017). Bank Solvency and Funding Cost: New Data and New Results, International Monetary Fund WP No. 17/116.

Shin C. and M. White (2020). "Fire-Sale Vulnerabilities of Banks: Bank-Specific Risks under Stress and Credit Drawdowns," FEDS Notes. Washington: Board of Governors of the Federal Reserve System, October 08, 2020, Available at Link.

Shin, H.S. (2009), "Reflections on Northern Rock: The Bank Run That Heralded the Global Financial Crisis", *Journal of Economic Perspectives*, 23(1):101-119

Standard & Poor (2024), "Default, Transition, and Recovery: 2023 Annual Global Corporate Default And Rating Transition Study", 28th Mrach, 2024. Retrieved from: Link.

Sydow M., A. Schilte, G. Covi, M. Deipenbrock, L. Del Vecchio, P. Fiedor, G. Fukker, M. Gehrend, R. Gourdel, A. Grassi, B. Hilberg, M. Kaijser, G. Kaoudis, L. Mingarelli, M. Montagna, T. Piquard, D. Salakhova, and N. Tente (2024), "Shock amplification in an interconnected financial system of banks and investment funds", *Journal of Financial Stability* 71

Upper, C. (2011), "Simulation methods to assess the danger of contagion in interbank markets", *Journal of Financial Stability*, 7(3):111-125.

Van den Heuvel S.J. (2002), "Does bank capital matter for monetary transmission", Federal Reserve Bank of New York, *Economic Policy Review* 9(1): 258-265

Van Oordt M.R.C. (2023), "Calibrating the magnitude of the countercyclical capital buffer using market-based stress tests", *Journal of Money, Credit and Banking* 55(2):465-501

Vazquez F. and P. Federico (2015), "Bank funding structures and risk: evidence from the global financial crisis", *Journal of Banking and Finance* 61:1-14

## Appendix A - Correlated Firm Default

To model counterparty default events we rely on a Monte Carlo sampling method modelling the dependence structure of counterparty defaults across sectors and countries via a Gaussian copula model (Glasserman, 2004; Glasserman and Li, 2005). Correlated default events as discussed in Acemoglu et al. (2012, 2015) as well as in Gabaix (2011) may be generated via

intersectoral input-output linkages (supply chain spillovers) that is, via common country and sector-specific financial and macro shocks. This interdependence among obligors' default is introduced through a multivariate normal vector ($\xi 1, \ldots, \xi j$) of latent variables. Each default indicator is represented as:

$$Y_j = 1\{\xi j > x_j\},\ j = 1, \ldots, J.$$

The threshold $x_j$ represents the default boundary (Merton, 1974), which is matched to the marginal default probability of obligor j ($PD_j$). $\xi j$ follow a standard normal distribution and we set $x_j = \varphi^{-1}(1 - PD_j)$, where $\varphi$ is the cumulative normal distribution, and the correlations among the $\xi j$ determine the dependence among the $Y_j$ as follows:

$$P(Y_j = 1) = P(\xi j > x_j) = P(\xi j > \varphi^{-1}(1 - PD_j) = PD_j$$

To derive the set of obligors' default indicator $Y_j$, we estimate the correlation structure of $\xi j$ which estimated using historical probability of defaults by country-sector pair following Covi et al, (2022), Covi et. (2024). In this respect, we estimate a correlation structure or dependence structure of corporate defaults across all sector (4) and country (134) pairs. We estimate this dependence structure as time-invariant correlation structure of probability of defaults over the period Q1-2015 to Q1-2024. Figure A1 summarizes the distribution of correlation coefficients for all sector-country pairs, which resembles a normal distribution, with a positive mean/median coefficient close 0.014. This feature implies that shocks to corporates (default events) can be to the same extent positive or negative correlated, reflecting the heterogeneous effects of macro and financial shocks across sectors and countries.

Figure A1: Obligors' Dependence Structure for Sector-Country Pairs

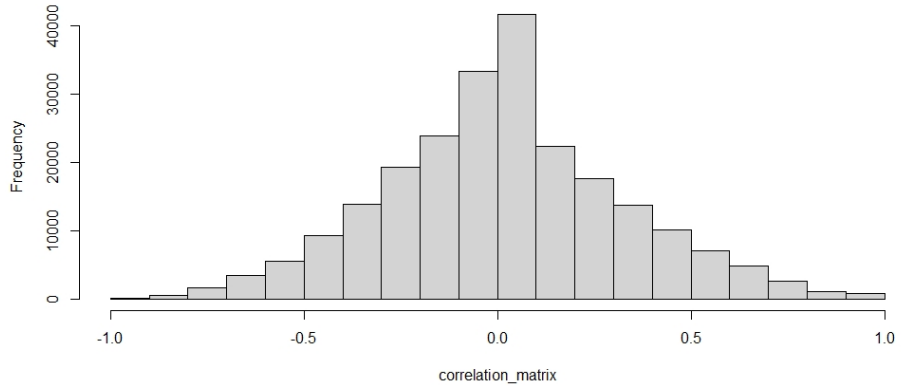


*Source: Supervisory COREP Data C09.02*

## Appendix B – Balance Sheet Accounting

Starting balance sheets (S=0) are collected from stress testing and supervisory COREP and FINREP templates. Step1 (S=1) consists in deriving the distribution of a firm's balance sheet (across n simulations) conditional to the estimated stochastic profit and loss shocks ($PL^{EC}_{i,n,t}$). In this respect, we adjust banks' risk-weighted assets ($RWA^{1}_{i,n,t}$) by the P&L shock ($PL^{EC}_{i,n,t}$)

which is proxied by an average bank/time-specific risk weight calculated as $(\frac{RWA^0_{i,t}}{TA^0_{i,t}})$[50]. Subsequently, we update the networks of loan ($L^1_{i,j,n,t}$), security ($S^1_{i,j,n,t}$) and funding exposures ($F^1_{i,j,n,t}$).

**Post Initial Shock - Block 1**

$$TA^1_{i,n,t} = TA^0_{i,t} + PL_{i,n,t} \quad ; \quad RWA^1_{i,n,t} = RWA^0_{i,t} + \left(PL_{i,n,t} * \frac{RWA^0_{i,t}}{TA^0_{i,t}}\right)$$

$$Cash^1_{i,n,t} = Cash^0_{i,t} - F_{i,n,t} \quad , \quad Cash\_Buffer^1_{i,n,t} = Cash\_Buffer_{i,t} \; - \; F_{i,n,t}$$

$$CET1^1_{i,n,t} = CET1^0_{i,t} + PL_{i,n,t} \quad , \quad CET1r^1_{i,n,t} = \frac{CET1^1_{i,n,t}}{RWA^1_{i,n,t}}$$

$$TIER1^1_{i,n,t} = TIER1^0_{i,t} + PL_{i,n,t} \quad , \quad LR^1_{i,n,t} = \frac{TA^1_{i,n,t} - CASH^1_{i,n,t}}{TIER1^1_{i,n,t}}$$

$$NTW^1_{i,j,n,t} = NTW_{i,j,t} \; - \; NTW_{i,j,t} | CP_{i,n,t} = 1 \; with \; NTW \in [Loan, Funding, Security]$$

**Post Funding Cost - Block 2**

$$TA^3_{i,n,t} = TA^1_{i,n,t} + \left(B^S_{i,n,t} + \quad B^U_{i,n,t}\right) - \; FC_{i,n,t} \quad , \quad RWA^3_{i,n,t} \; = \; RWA^1_{i,n,t}$$

$$Cash^2_{i,n,t} = Cash_{i,t} - \; F^2_{i,n,t} \quad , \quad Cash^3_{i,n,t} = Cash_{i,t} - \; F^2_{i,n,t} + \left(B^S_{i,n,t} + \quad B^U_{i,n,t}\right) - \; FC_{i,n,t}$$

$$CET1^3_{i,n,t} = CET1^1_{i,t} - \; FC_{i,n,t} \quad , \quad CET1r^3_{i,n,t} = \frac{CET1^3_{i,n,t}}{RWA^3_{i,n,t}}$$

$$TIER1^3_{i,n,t} = TIER1^1_{i,t} - \; FC_{i,n,t} \quad , \quad LR^1_{i,n,t} = \frac{TA^1_{i,n,t} - CASH^1_{i,n,t}}{TIER1^1_{i,n,t}}$$

$$SEC^3_{i,n,t} = SEC^1_{i,n,t} - \; B^S_{i,n,t} \quad , \quad SEC\_HQLA^3_{i,n,t} = HQLA^1_{i,n,t} - \; B^S_{i,n,t}$$

**Post Fire Sale Shock - Block 3**

$$TA^4_{i,n,t} = TA^3_{i,n,t} - FS_{i,n,t}$$

$$RWA^4_{i,n,t} = \; RWA^3_{i,n,t} - \left(Q^{***}_{i,n,t} * \frac{RWA^0_{i,t}}{TA^0_{i,t}} * \left(1 - \; HQLA\_share^3_{i,t}\right)\right)$$

[50] This assumption leads us to conservative regulatory ratio estimates (CET1r) since the methodology by construction overestimate post shock RWAs especially in the tail of P&L distribution. More risky obligors (with high probability of default) default more often compared to less risky obligors (with low probability of defaults), thereby determining this overestimation RWA bias. Nonetheless, in this way we address the critique posed by Acharya et al. (2014) which highlight that banks may underestimate their risk-weights given the average risk weight appears unconnected with their actual risk.

$$CET1^{3}_{i,n,t} = CET1^{1}_{i,n,t} - FS_{i,n,t} \quad , \quad CET1r^{3}_{i,n,t} = \frac{CET1^{3}_{i,n,t}}{RWA^{3}_{i,n,t}}$$

$$TIER1^{3}_{i,n,t} = TIER1^{1}_{i,n,t} - FS_{i,n,t} \, , \quad LR^{3}_{i,n,t} = \frac{TA^{3}_{i,n,t} - CASH^{3}_{i,n,t}}{TIER1^{3}_{i,n,t}}$$

$$Cash^{4}_{i,n,t} = Cash^{3}_{i,n,t} + (Q^{***}_{i,n,t} - FS_{i,n,t})$$

$$LR^{4}_{i,n,t} = \frac{TA^{4}_{i,n,t} - Cash^{4}_{i,n,t}}{TIER1^{4}_{i,n,t}}$$

$$SEC^{4}_{i,n,t} = SEC^{3}_{i,n,t} - (Q^{***}_{i,n,t} + FS_{i,n,t})$$

$$SEC\_HQLA^{4}_{i,n,t} = HQLA^{3}_{i,n,t} - (Q^{***|HQLA}_{i,n,t} + FS^{HQLA}_{i,n,t})$$

**Appendix C - Regulatory Constraints**

$$Solvency\ Default: DF^{CET1}_{i,n,t} = 1\ if\ CET1r_{i,n,t} < CET1r\ Minima$$

Where: $CET1r\ Minima = 6.5\%\ RWAs$

$$Leverage\ Default: DF^{LEV}_{i,n,t} = 1\ if\ LR_{i,n,t} < LR\ Minima$$

Where: $LR\ Minima = 31 * TIER1\ Capital$

$$Liquidity\ Default: DF^{LIQ}_{i,n,t} = 1\ if\ \ LIQ_{i,n,t} = \ CASH_{i,n,t} + \ HQLA_{i,n,t} < Funding\ Needs_{i,n,t}$$

$$Solvency\ Distress: DS^{CET1}_{i,n,t} = 1\ if\ CET1r\ Minima\ < CET1r_{i,n,t} < CET1\ Buffer$$

Where: $CET1\ Buffer\ = 11\%\ RWAs$

$$Leverage\ Distress: DS^{LEV}_{i,n,t} = 1\ if\ LR\ Minima\ <\ LR_{i,n,t} < LR\ Buffer$$

Where: $LR\ Minima = 25 * TIER1\ Capital$

$$Liquidity\ Distress: DS^{LIQ}_{i,n,t} = 1\ if\ \ CASH\ Buffer_{i,n,t} < 0\ \ \&\ \ DF^{LIQ}_{i,n,t} = 0$$

**Appendix D –Supply and Demand of Funding**

<u>Supply</u>

As the system supply depends on the severity of each realisation, the initial values of $a^{(un)sec}_{i,t}$ in equation (3c) are modelled based on rescaling the system funding shock that is given in each quarter and scenario, such that is in line with previously mentioned empirical findings: in case

of a negative shock, the volume on secured market increases, whereas opposite is true on the unsecured market. Since both the supply and demand vary at each realisation, depending on bank and system-specific characteristics, and need to intersect in order to obtain optimal quantities, the available supply will be different compared to the realised one. Table D.1. shows this for the case of secured market, whereas the unsecured one is shown in Table D.2.

Table D.1. Possible and realised secured supply, in billion £

| date | Possible | | | | | | | | |
|---|---|---|---|---|---|---|---|---|---|
| | min sec | 1% | 2.50% | 5% | 50% | 95% | 97.50% | 99% | max sec |
| 31-Dec-19 | 80.00 | 80.02 | 80.03 | 80.14 | 80.51 | 85.03 | 88.02 | 95.00 | 130.00 |
| 31-Mar-20 | 80.00 | 80.02 | 80.03 | 80.14 | 80.53 | 87.35 | 91.52 | 97.52 | 130.00 |
| 30-Jun-20 | 80.00 | 80.02 | 80.03 | 80.14 | 80.65 | 86.35 | 90.52 | 96.19 | 130.00 |
| 30-Sep-20 | 80.00 | 80.02 | 80.03 | 80.14 | 80.64 | 86.31 | 90.47 | 95.69 | 130.00 |
| 31-Dec-20 | 80.00 | 80.02 | 80.03 | 80.15 | 80.68 | 87.16 | 91.33 | 97.83 | 130.00 |
| 31-Mar-21 | 80.00 | 80.02 | 80.03 | 80.14 | 80.64 | 86.67 | 90.82 | 98.14 | 130.00 |
| 30-Jun-21 | 80.00 | 80.02 | 80.02 | 80.13 | 80.53 | 86.51 | 90.36 | 97.13 | 130.00 |
| 30-Sep-21 | 80.00 | 80.02 | 80.13 | 80.15 | 80.68 | 87.48 | 91.98 | 98.19 | 130.00 |
| 31-Dec-21 | 80.00 | 80.02 | 80.03 | 80.14 | 80.68 | 87.33 | 91.98 | 98.31 | 130.00 |
| 31-Mar-22 | 80.00 | 80.02 | 80.03 | 80.15 | 80.64 | 86.31 | 90.64 | 96.64 | 130.00 |
| 30-Jun-22 | 80.00 | 80.03 | 80.14 | 80.15 | 80.53 | 85.85 | 90.17 | 96.15 | 130.00 |
| 30-Sep-22 | 80.00 | 80.02 | 80.14 | 80.15 | 80.66 | 86.18 | 89.97 | 94.63 | 130.00 |
| 31-Dec-22 | 80.00 | 80.03 | 80.14 | 80.16 | 80.80 | 86.19 | 90.85 | 95.99 | 130.00 |
| 31-Mar-23 | 80.00 | 80.02 | 80.14 | 80.15 | 80.69 | 86.35 | 90.36 | 95.51 | 130.00 |
| 30-Jun-23 | 80.00 | 80.03 | 80.14 | 80.15 | 80.67 | 85.66 | 89.16 | 94.66 | 130.00 |
| 30-Sep-23 | 80.00 | 80.02 | 80.14 | 80.15 | 80.81 | 86.83 | 90.85 | 98.15 | 130.00 |
| 31-Dec-23 | 80.00 | 80.03 | 80.14 | 80.15 | 80.69 | 85.65 | 88.85 | 94.87 | 130.00 |
| 31-Mar-24 | 80.00 | 80.03 | 80.14 | 80.16 | 80.82 | 86.14 | 90.02 | 96.50 | 130.00 |

| date | Realised | | | | | | | | |
|---|---|---|---|---|---|---|---|---|---|
| | min sec | 1% | 2.50% | 5% | 50% | 95% | 97.50% | 99% | max sec |
| 31-Dec-19 | 0.05 | 0.21 | 0.28 | 0.37 | 1.85 | 17.21 | 27.21 | 50.75 | 130.00 |
| 31-Mar-20 | 0.08 | 0.28 | 0.38 | 0.51 | 2.32 | 28.90 | 45.26 | 68.53 | 130.00 |
| 30-Jun-20 | 0.08 | 0.25 | 0.34 | 0.46 | 2.28 | 22.91 | 37.87 | 58.25 | 130.00 |
| 30-Sep-20 | 0.03 | 0.21 | 0.29 | 0.40 | 2.07 | 21.28 | 35.34 | 53.32 | 130.00 |
| 31-Dec-20 | 0.07 | 0.26 | 0.36 | 0.47 | 2.50 | 24.93 | 39.43 | 61.70 | 130.00 |
| 31-Mar-21 | 0.04 | 0.22 | 0.29 | 0.37 | 2.22 | 24.36 | 39.41 | 65.65 | 130.00 |
| 30-Jun-21 | 0.05 | 0.19 | 0.25 | 0.34 | 2.06 | 23.03 | 36.65 | 60.03 | 130.00 |
| 30-Sep-21 | 0.04 | 0.17 | 0.22 | 0.29 | 1.52 | 16.11 | 25.81 | 38.88 | 98.81 |
| 31-Dec-21 | 0.07 | 0.17 | 0.23 | 0.30 | 1.58 | 15.81 | 25.79 | 38.95 | 98.59 |
| 31-Mar-22 | 0.07 | 0.24 | 0.32 | 0.41 | 1.93 | 19.28 | 32.53 | 50.89 | 130.00 |
| 30-Jun-22 | 0.06 | 0.30 | 0.39 | 0.50 | 2.15 | 21.75 | 37.60 | 59.61 | 130.00 |
| 30-Sep-22 | 0.11 | 0.28 | 0.38 | 0.49 | 2.08 | 18.92 | 30.19 | 44.32 | 130.00 |
| 31-Dec-22 | 0.05 | 0.23 | 0.31 | 0.41 | 1.98 | 16.03 | 28.01 | 41.18 | 119.71 |
| 31-Mar-23 | 0.07 | 0.22 | 0.29 | 0.39 | 1.86 | 15.90 | 25.88 | 38.60 | 115.11 |
| 30-Jun-23 | 0.04 | 0.19 | 0.26 | 0.34 | 1.58 | 13.18 | 21.25 | 34.01 | 107.10 |
| 30-Sep-23 | 0.07 | 0.19 | 0.25 | 0.34 | 1.70 | 14.26 | 22.68 | 37.39 | 95.15 |
| 31-Dec-23 | 0.05 | 0.21 | 0.28 | 0.36 | 1.75 | 13.42 | 21.09 | 35.44 | 109.69 |
| 31-Mar-24 | 0.04 | 0.21 | 0.27 | 0.34 | 1.68 | 12.48 | 20.56 | 33.73 | 93.10 |

Table D.2. Possible and realised unsecured supply, in billion £

| date | Possible | | | | | | | | |
|---|---|---|---|---|---|---|---|---|---|
| | **max unsec** | **1%** | **2.50%** | **5%** | **50%** | **95%** | **97.50%** | **99%** | **min unsec** |
| 31-Dec-19 | 50.11 | 47.98 | 47.97 | 47.95 | 47.88 | 46.76 | 46.08 | 42.68 | 23.00 |
| 31-Mar-20 | 50.11 | 47.98 | 47.96 | 48.00 | 47.86 | 46.22 | 45.23 | 41.52 | 23.00 |
| 30-Jun-20 | 50.11 | 47.98 | 47.96 | 48.00 | 47.84 | 46.47 | 45.48 | 42.09 | 23.00 |
| 30-Sep-20 | 50.11 | 47.97 | 47.96 | 48.00 | 47.85 | 46.51 | 45.49 | 42.38 | 23.00 |
| 31-Dec-20 | 50.11 | 47.97 | 47.96 | 47.99 | 47.85 | 46.28 | 45.29 | 41.36 | 23.00 |
| 31-Mar-21 | 50.11 | 47.98 | 47.97 | 47.95 | 47.85 | 46.42 | 45.40 | 42.30 | 23.00 |
| 30-Jun-21 | 50.11 | 47.98 | 47.97 | 47.96 | 47.86 | 46.43 | 45.50 | 42.27 | 23.00 |
| 30-Sep-21 | 50.11 | 47.97 | 47.96 | 47.99 | 47.86 | 46.22 | 45.12 | 42.11 | 23.00 |
| 31-Dec-21 | 50.11 | 47.98 | 47.96 | 48.00 | 47.85 | 46.24 | 45.12 | 41.60 | 23.00 |
| 31-Mar-22 | 50.11 | 47.97 | 47.96 | 47.99 | 47.85 | 46.51 | 45.45 | 42.17 | 23.00 |
| 30-Jun-22 | 50.11 | 47.97 | 47.95 | 47.99 | 47.87 | 46.61 | 45.57 | 42.28 | 23.00 |
| 30-Sep-22 | 50.11 | 47.97 | 47.95 | 47.99 | 47.83 | 46.50 | 45.64 | 42.24 | 23.00 |
| 31-Dec-22 | 50.11 | 47.97 | 48.00 | 47.98 | 47.82 | 46.49 | 45.42 | 42.25 | 23.00 |
| 31-Mar-23 | 50.11 | 47.97 | 47.95 | 47.99 | 47.84 | 46.46 | 45.50 | 42.67 | 23.00 |
| 30-Jun-23 | 50.11 | 47.97 | 47.95 | 47.99 | 47.82 | 46.62 | 45.83 | 43.48 | 23.00 |
| 30-Sep-23 | 50.11 | 47.97 | 47.96 | 47.99 | 47.81 | 46.34 | 45.37 | 41.97 | 23.00 |
| 31-Dec-23 | 50.11 | 47.97 | 47.95 | 47.99 | 47.84 | 46.63 | 45.87 | 43.21 | 23.00 |
| 31-Mar-24 | 50.11 | 47.96 | 48.00 | 47.98 | 47.80 | 46.55 | 45.57 | 42.92 | 23.00 |

| date | Realised | | | | | | | | |
|---|---|---|---|---|---|---|---|---|---|
| | **min unsec** | **1%** | **2.50%** | **5%** | **50%** | **95%** | **97.50%** | **99%** | **max unsec** |
| 31-Dec-19 | 0.02 | 0.11 | 0.15 | 0.20 | 1.00 | 9.27 | 14.61 | 26.47 | 42.06 |
| 31-Mar-20 | 0.04 | 0.15 | 0.21 | 0.27 | 1.25 | 15.56 | 23.92 | 35.88 | 42.76 |
| 30-Jun-20 | 0.04 | 0.14 | 0.18 | 0.25 | 1.23 | 12.34 | 20.06 | 30.37 | 42.41 |
| 30-Sep-20 | 0.02 | 0.12 | 0.16 | 0.21 | 1.12 | 11.46 | 18.71 | 27.77 | 42.50 |
| 31-Dec-20 | 0.04 | 0.14 | 0.19 | 0.25 | 1.35 | 13.42 | 20.81 | 32.21 | 42.23 |
| 31-Mar-21 | 0.02 | 0.12 | 0.15 | 0.20 | 1.19 | 13.12 | 20.86 | 34.34 | 42.63 |
| 30-Jun-21 | 0.03 | 0.10 | 0.14 | 0.18 | 1.11 | 12.40 | 19.42 | 31.28 | 42.31 |
| 30-Sep-21 | 0.02 | 0.09 | 0.12 | 0.16 | 0.82 | 8.68 | 13.40 | 19.93 | 38.97 |
| 31-Dec-21 | 0.04 | 0.09 | 0.12 | 0.16 | 0.85 | 8.51 | 13.39 | 19.97 | 38.92 |
| 31-Mar-22 | 0.04 | 0.13 | 0.17 | 0.22 | 1.04 | 10.38 | 17.18 | 26.36 | 41.67 |
| 30-Jun-22 | 0.03 | 0.16 | 0.21 | 0.27 | 1.16 | 11.71 | 19.95 | 31.11 | 42.52 |
| 30-Sep-22 | 0.06 | 0.15 | 0.21 | 0.26 | 1.12 | 10.19 | 16.00 | 23.06 | 41.45 |
| 31-Dec-22 | 0.03 | 0.12 | 0.17 | 0.22 | 1.07 | 8.63 | 14.71 | 21.20 | 40.55 |
| 31-Mar-23 | 0.04 | 0.12 | 0.16 | 0.21 | 1.00 | 8.56 | 13.62 | 19.87 | 40.07 |
| 30-Jun-23 | 0.02 | 0.10 | 0.14 | 0.18 | 0.85 | 7.10 | 11.27 | 17.50 | 39.51 |
| 30-Sep-23 | 0.04 | 0.10 | 0.14 | 0.18 | 0.91 | 7.68 | 11.84 | 19.13 | 39.31 |
| 31-Dec-23 | 0.03 | 0.11 | 0.15 | 0.19 | 0.94 | 7.22 | 11.22 | 18.24 | 39.74 |
| 31-Mar-24 | 0.02 | 0.11 | 0.14 | 0.19 | 0.90 | 6.72 | 10.80 | 17.13 | 38.12 |

Finally, table D.3. shows how the share of unsecured supply decreases as the size of the shock increases, which is described in the main text. Our modelling approach captures this feature.

Table D.3. Share of unsecured demand

| date | **Possible unsecured share in %** | | | | | | | | |
|---|---|---|---|---|---|---|---|---|---|
| | **max unsec** | **1%** | **2.50%** | **5%** | **50%** | **95%** | **97.50%** | **99%** | **min unsec** |
| 31-Dec-19 | 38.51 | 37.48 | 37.47 | 37.44 | 37.29 | 35.48 | 34.36 | 31.00 | 15.03 |
| 31-Mar-20 | 38.51 | 37.48 | 37.47 | 37.46 | 37.28 | 34.60 | 33.07 | 29.86 | 15.03 |
| 30-Jun-20 | 38.51 | 37.48 | 37.47 | 37.46 | 37.24 | 34.99 | 33.44 | 30.44 | 15.03 |
| 30-Sep-20 | 38.51 | 37.48 | 37.47 | 37.46 | 37.24 | 35.02 | 33.46 | 30.69 | 15.03 |
| 31-Dec-20 | 38.51 | 37.48 | 37.47 | 37.45 | 37.23 | 34.68 | 33.15 | 29.71 | 15.03 |

| | | | | | | | | | |
|---|---|---|---|---|---|---|---|---|---|
| 31-Mar-21 | 38.51 | 37.48 | 37.48 | 37.44 | 37.24 | 34.88 | 33.33 | 30.12 | 15.03 |
| 30-Jun-21 | 38.51 | 37.49 | 37.48 | 37.44 | 37.28 | 34.93 | 33.49 | 30.32 | 15.03 |
| 30-Sep-21 | 38.51 | 37.48 | 37.44 | 37.45 | 37.23 | 34.57 | 32.91 | 30.01 | 15.03 |
| 31-Dec-21 | 38.51 | 37.48 | 37.47 | 37.46 | 37.23 | 34.62 | 32.91 | 29.73 | 15.03 |
| 31-Mar-22 | 38.51 | 37.48 | 37.47 | 37.45 | 37.24 | 35.02 | 33.40 | 30.38 | 15.03 |
| 30-Jun-22 | 38.51 | 37.48 | 37.44 | 37.45 | 37.28 | 35.19 | 33.57 | 30.54 | 15.03 |
| 30-Sep-22 | 38.51 | 37.48 | 37.44 | 37.45 | 37.22 | 35.04 | 33.66 | 30.86 | 15.03 |
| 31-Dec-22 | 38.51 | 37.47 | 37.46 | 37.44 | 37.18 | 35.04 | 33.33 | 30.56 | 15.03 |
| 31-Mar-23 | 38.51 | 37.48 | 37.44 | 37.45 | 37.22 | 34.98 | 33.49 | 30.88 | 15.03 |
| 30-Jun-23 | 38.51 | 37.48 | 37.44 | 37.45 | 37.22 | 35.24 | 33.95 | 31.47 | 15.03 |
| 30-Sep-23 | 38.51 | 37.48 | 37.44 | 37.45 | 37.17 | 34.80 | 33.31 | 29.95 | 15.03 |
| 31-Dec-23 | 38.51 | 37.48 | 37.44 | 37.45 | 37.22 | 35.25 | 34.05 | 31.29 | 15.03 |
| 31-Mar-24 | 38.51 | 37.47 | 37.46 | 37.44 | 37.16 | 35.08 | 33.61 | 30.79 | 15.03 |

| **date** | **Realised unsecured share in %** | | | | | | | | |
|---|---|---|---|---|---|---|---|---|---|
| | **max unsec** | **1%** | **2.50%** | **5%** | **50%** | **95%** | **97.50%** | **99%** | **min unsec** |
| 31-Dec-19 | 34.78 | 35.09 | 35.01 | 34.94 | 34.99 | 35.00 | 34.94 | 34.28 | 24.45 |
| 31-Mar-20 | 34.92 | 34.99 | 34.97 | 35.04 | 35.01 | 35.00 | 34.58 | 34.36 | 24.75 |
| 30-Jun-20 | 34.92 | 35.05 | 34.91 | 35.01 | 34.99 | 35.00 | 34.63 | 34.27 | 24.60 |
| 30-Sep-20 | 34.88 | 34.95 | 35.04 | 35.02 | 35.01 | 35.00 | 34.62 | 34.25 | 24.64 |
| 31-Dec-20 | 35.14 | 35.00 | 35.02 | 34.99 | 34.99 | 35.00 | 34.54 | 34.30 | 24.52 |
| 31-Mar-21 | 35.00 | 35.03 | 35.00 | 34.96 | 35.01 | 35.00 | 34.61 | 34.34 | 24.69 |
| 30-Jun-21 | 35.21 | 34.97 | 35.05 | 34.92 | 35.00 | 35.00 | 34.63 | 34.26 | 24.56 |
| 30-Sep-21 | 34.48 | 35.16 | 35.10 | 34.99 | 35.00 | 35.00 | 34.17 | 33.89 | 28.28 |
| 31-Dec-21 | 34.95 | 34.98 | 35.13 | 34.90 | 34.99 | 35.00 | 34.17 | 33.89 | 28.30 |
| 31-Mar-22 | 34.65 | 35.05 | 34.96 | 35.02 | 35.01 | 35.00 | 34.55 | 34.12 | 24.27 |
| 30-Jun-22 | 35.29 | 35.02 | 35.05 | 34.97 | 35.00 | 35.00 | 34.67 | 34.29 | 24.65 |
| 30-Sep-22 | 34.97 | 35.05 | 35.03 | 35.01 | 34.99 | 35.00 | 34.63 | 34.22 | 24.18 |
| 31-Dec-22 | 35.14 | 34.94 | 35.00 | 35.01 | 35.00 | 35.00 | 34.44 | 33.99 | 25.30 |
| 31-Mar-23 | 34.62 | 35.03 | 34.96 | 35.01 | 35.00 | 35.00 | 34.48 | 33.98 | 25.82 |
| 30-Jun-23 | 34.43 | 34.97 | 34.95 | 35.01 | 34.99 | 35.00 | 34.66 | 33.98 | 26.95 |
| 30-Sep-23 | 34.91 | 35.05 | 35.05 | 34.95 | 34.99 | 35.00 | 34.30 | 33.84 | 29.24 |
| 31-Dec-23 | 35.37 | 35.02 | 34.98 | 34.96 | 35.00 | 35.00 | 34.72 | 33.98 | 26.59 |
| 31-Mar-24 | 35.38 | 35.13 | 34.95 | 35.04 | 34.98 | 35.00 | 34.43 | 33.68 | 29.05 |

We report the distributions of the (un)secured supplies and how they change in normal versus stressful times. We plot histograms in figures D.1 and D.2. of possible supplies derived in the model, based on all realisations and all quarters of the analysis. The substitution effects between the two times and markets are apparent.

Figure D.1. Secured supply quantity, histogram

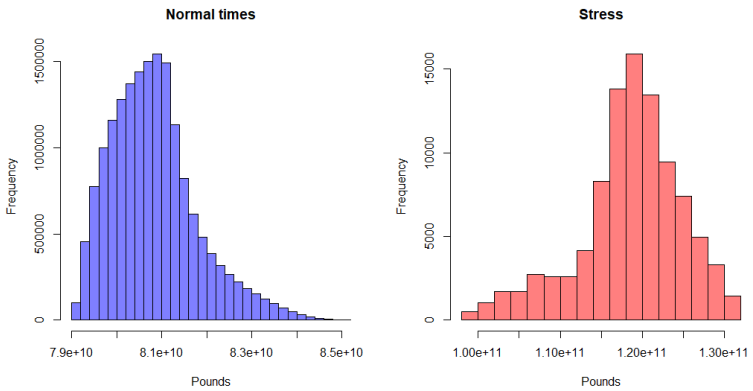

Figure D.2. Unsecured supply quantity, histogram

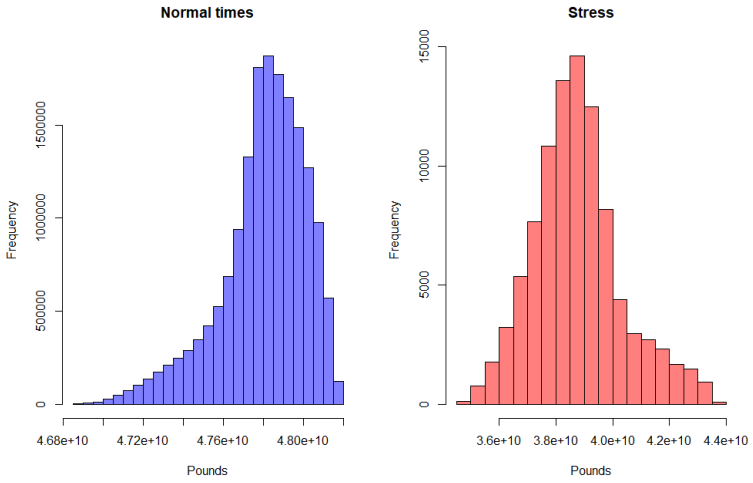


*Demand*

To estimate demands on (un)secured market, $D_{n,t}^{(un)sec} = c_{i,t}^{(un)sec} - d \cdot spread_{n,t}^{(un)sec}$, $d > 0$, we obtain initial values of system demand $c_{i,t}^{(un)sec}$, such that that the actual liquidity that remains after the shock is regressed on the size of the funding shock, in line with the cointegrating relationship between required and actual liquidity modelled in Dujim and Wierts (2016). By doing so, we obtain higher positive values of demand in case of worst funding shocks, whereas in good times, resulting demand becomes negligible. Finally, the coefficients *b* and *d* in supply and demand equations are kept constant across different realisations, which means that the slope of all curves does not change. In the end, we have 10.000 upward sloping functions of supply curves which shift at quarter, with shifting to right (left) when realizations are worse for the secured (unsecured) case, and to the right (left) when realizations are better than the median.

## Appendix E – Cost of Funding

Cost of funding for each bank as described in the main text, depends on the own riskiness, the overall market risk, and central bank rate. Figure E.1. shows the full range of potential Cost of Funding outcomes in our framework, respectively for the secured and unsecured markets. As the secured and unsecured spreads are very similar with respect to their upper and lower bound, the resulting overall cost of funding on both markets is similar, with a bit greater value for the unsecured market. Figure E.2. (left panel) shows the satisfied quantities on both markets, and (right panel) the resulting cost of funding in monetary units.

Figure E.1. Cost of funding, secured market – left panel, unsecured market – right panel

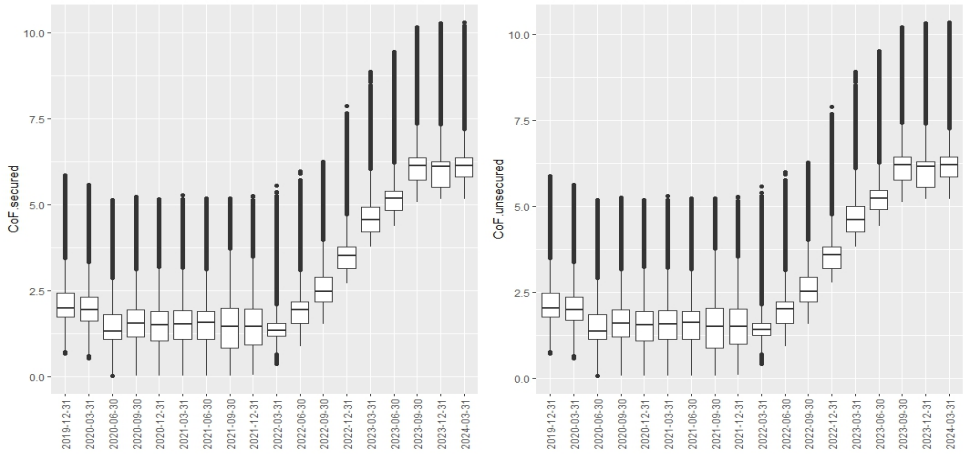


Figure E.2. Satisfied quantities on both markets (left panel) and cost of funding in monetary units (right panel)

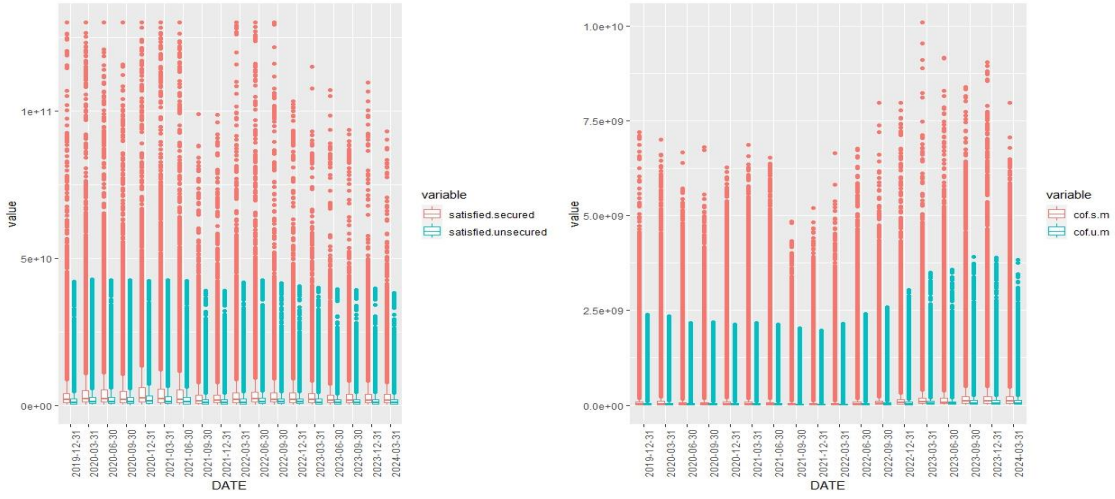

## Appendix F – selected bank runs

| Bank, date | % of deposits, time | Reason | Source |
|---|---|---|---|
| Banking System, Saudi Arabia, 1990 | 11%, 1 week | Political uncertainty, after invasion of Kuwait by Iraq | Schmeider et al. (2011) |
| Banesto, Spain, 1994 | 8%, 1 week | Bad business choices ("disastrous expansion of loan book"); central bank took control, loss of confidence | Schmeider et al. (2011); Counsel (1994) |
| Banking System, Argentina, 2001 | 30%, 9 months | Economic crisis resulted in loss of confidence | McCandless et al. (2003) |
| Banking System, Uruguay, 2002 | 56%, 6 months | Spread from Argentina (dependent on Arg) | Schmeider et al. (2011) |
| Northern rock, UK, 2007 | 57%, 12 months | After announcement about using emergency loan facility of BoE, depositors made a bank run | Shin (2009) |
| Parex bank, Latvia, 2008 | 25%, 4 months | FCMC[51] revealed shortcomings in the lending process (i.e. bad business conduct), loss of confidence | IMF (2013) |
| IndyMac bank, USA, 2008 | 7.5%, 1 week | After Senator Schumer released letters he sent to regulators about bank's problems[52] | FDIC (2009) |
| DSB bank, Netherlands, 2009 | 30%, 12 days | Business choice of selling mortgages jointly with life insurance led to high premiums that customers were not able to cope with. This led to founding a foundation of unsatisfied customers, whose representative P. Lakeman motivated depositors to make a bank run. | Pruyt & Hamart (2010) |
| Metro bank, UK, 2019 | Not estimated | Social media rumour spread, after a fall of the bank's stock price | Bloomberg (2019) |
| Sberbank Europe AG, Austria, 2022<br>Sberbank branch/subsidiary Czech Republic, Croatia, Slovenia, 2022 | Not estimated yet, runs lasted a couple of days | Geopolitical events, loss of confidence in the bank | EBA (2022)<br>EBA (2022b) |
| SVB, US, 2023 | 25%, 1 day | Explained in main body of the paper | FED (2023) |
| Signature Bank, US, 2023 | 20%, 1 day | | |
| First Republic, US, 2023 | 57%, 7-14 days | | |

[51] Financial and Capital Market Commission of Latvia

[52] Due to bank relying "heavily on higher cost, less stable, brokered deposits, as well as secured borrowings, to fund its operations and focused on stated income and other aggressively underwritten loans in areas with rapidly escalating home prices, particularly in California and Florida".

## Appendix G – Robustness Checks

Figure G1 – Loss Impact of Management Actions by Round

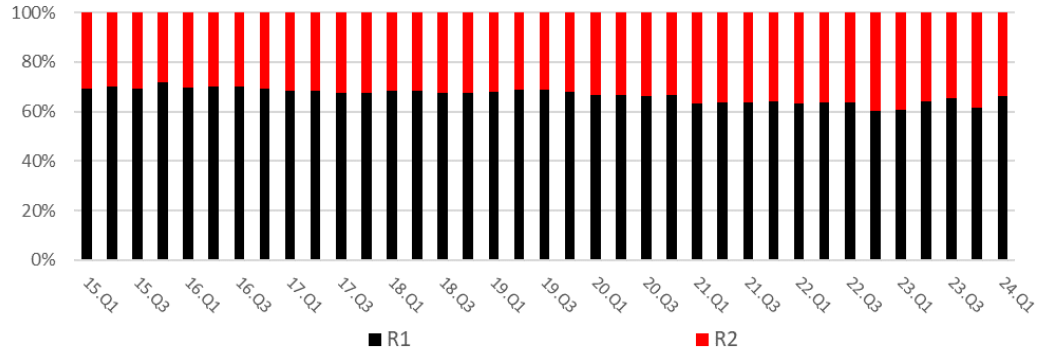


Note: R1 refers to the Round 1 and R2 refers to Round 2 effects.

Table G2 – Correlation Funding Shocks and Losses by percentile

| **Correlation** | Fund Shock1 - Initial Losses | Fund Shock2 - Initial Losses | Fund Shock3 - Total Loss |
|---|---|---|---|
| pct99 | 0.37 | 0.54 | 0.43 |
| pct95 | 0.42 | 0.45 | 0.14 |
| pct90 | 0.67 | 0.68 | 0.11 |

Note: Fund Shock1 refers to initial funding shocks, fund shock2 to funding withdrawals augmented with Round 1 bank runs, and fund shock3 to funding withdrawals augmented with Round 1 and Round 2 bank runs.

Table G3: Funding Cost Channel Sensitivity to Stress Horizon and Funding Shock Size (Basis Points)

| **Delta PD** | **2015** | **2016** | **2017** | **2018** | **2019** | **2020** | **2021** | **2022** | **2023** | **2024** |
|---|---|---|---|---|---|---|---|---|---|---|
| PD_3M_10S | 0.1 | 0.1 | 0.1 | 0.0 | 0.1 | 0.0 | 0.0 | 0.0 | 0.0 | 0.0 |
| PD_3M_20S | 0.2 | 0.3 | 0.2 | 0.1 | 0.3 | 0.1 | 0.1 | 0.1 | 0.0 | 0.0 |
| PD_3M_30S | 0.4 | 0.5 | 0.2 | 0.2 | 0.4 | 0.2 | 0.1 | 0.1 | 0.4 | 0.0 |
| PD_3M_40S | 0.6 | 0.7 | 0.2 | 0.2 | 0.5 | 0.2 | 0.2 | 0.3 | 0.4 | 0.0 |
| PD_3M_50S | 1.1 | 1.0 | 0.2 | 0.3 | 0.6 | 0.2 | 0.2 | 0.3 | 0.4 | 0.0 |
| PD_6M | 1.9 | 1.9 | 0.5 | 0.9 | 0.8 | 0.5 | 0.2 | 0.5 | 0.6 | 0.0 |
| PD_6M_10S | 2.4 | 2.0 | 0.5 | 0.9 | 0.9 | 0.7 | 0.2 | 0.5 | 0.6 | 0.0 |
| PD_6M_20S | 2.9 | 2.4 | 0.5 | 1.1 | 1.3 | 0.7 | 0.2 | 0.5 | 0.7 | 0.0 |
| PD_6M_30S | 3.3 | 2.7 | 0.5 | 1.1 | 1.7 | 0.7 | 0.2 | 0.6 | 0.7 | 0.1 |
| PD_6M_40S | 3.8 | 3.2 | 0.9 | 1.2 | 1.8 | 0.7 | 0.2 | 0.7 | 0.9 | 0.1 |
| PD_6M_50S | 4.2 | 3.3 | 1.1 | 1.4 | 2.0 | 0.9 | 0.2 | 0.8 | 1.0 | 0.1 |
| PD_1Y | 6.3 | 4.7 | 2.2 | 2.2 | 2.8 | 1.6 | 0.4 | 1.6 | 1.5 | 0.9 |
| PD_1Y_10S | 7.0 | 5.8 | 2.3 | 2.4 | 3.2 | 2.0 | 0.8 | 1.9 | 1.7 | 0.9 |
| PD_1Y_20S | 7.8 | 6.6 | 2.5 | 2.7 | 3.2 | 2.0 | 0.8 | 2.0 | 1.9 | 1.4 |
| PD_1Y_30S | 9.0 | 7.4 | 2.7 | 3.0 | 3.7 | 2.1 | 1.1 | 2.1 | 2.3 | 1.4 |
| PD_1Y_40S | 10.0 | 8.2 | 3.1 | 3.4 | 4.0 | 2.3 | 1.5 | 2.4 | 2.3 | 1.4 |
| PD_1Y_50S | 10.9 | 8.6 | 3.8 | 3.6 | 4.4 | 2.6 | 1.6 | 2.7 | 2.6 | 1.5 |

Note: 3M, 6M and 1Y refer to the length of the stress horizon (baseline estimates are based on 3M), whereas 10S, 20S, 30S,40S, 50S to the severity of the funding shock increased respectively by 10% (10S) up to 50% (50S).

Table G4 – Average Probability of Default Decomposition by binding Default Thresholds

| PD Average | 2015 | 2016 | 2017 | 2018 | 2019 | 2020 | 2021 | 2022 | 2023 | 2024 |
|---|---|---|---|---|---|---|---|---|---|---|
| PD_CET_LEV | 80.6 | 73.8 | 44.8 | 62.4 | 73.9 | 106.2 | 71.1 | 55.9 | 40.3 | 41.0 |
| PD_CET | 83.6 | 54.0 | 56.2 | 69.1 | 13.6 | 12.5 | 6.3 | 2.5 | 5.0 | 7.3 |
| PD_LEV | 10.0 | 8.8 | 2.1 | 4.9 | 2.3 | 18.2 | 12.1 | 23.9 | 7.3 | 2.3 |
| PD_CET_LIQ | 2.3 | 3.5 | 3.4 | 2.1 | 0.0 | 0.5 | 1.3 | 0.4 | 0.0 | 0.0 |
| PD_LIQ | 0.2 | 0.2 | 0.2 | 0.0 | 0.0 | 0.0 | 0.0 | 0.0 | 0.0 | 0.0 |
| PD_CET_LEV_LIQ | 0.0 | 0.3 | 0.1 | 0.0 | 0.0 | 0.0 | 0.1 | 0.4 | 0.0 | 0.0 |
| PD_LEV_LIQ | 0.0 | 0.0 | 0.0 | 0.0 | 0.0 | 0.0 | 0.0 | 0.0 | 0.0 | 0.0 |
| TOT | 177 | 141 | 107 | 139 | 90 | 137 | 91 | 83 | 53 | 51 |

Table G5 – Average Probability of Default Sensitivity to CET1 Ratio Default Threshold

| | 2015 | 2016 | 2017 | 2018 | 2019 | 2020 | 2021 | 2022 | 2023 | 2024 | AVG |
|---|---|---|---|---|---|---|---|---|---|---|---|
| PD_6pct | 86 | 77 | 37 | 44 | 45 | 84 | 64 | 84 | 34 | 29 | 59 |
| **PD_7pct*** | **118** | **94** | **53** | **64** | **55** | **88** | **71** | **87** | **37** | **31** | **70** |
| PD_8pct | 180 | 144 | 79 | 89 | 81 | 104 | 94 | 101 | 48 | 46 | 97 |
| PD_9pct | 305 | 239 | 124 | 138 | 122 | 144 | 146 | 141 | 69 | 65 | 149 |
| PD_10pct | 517 | 386 | 190 | 209 | 183 | 215 | 213 | 211 | 106 | 98 | 233 |

Note: Xpct refers to the threshold used to identify a bank breaching its CET1 minimum capital requirements which was set equal to 7% across banks.

Figure G2 – US Banks' Default Rate

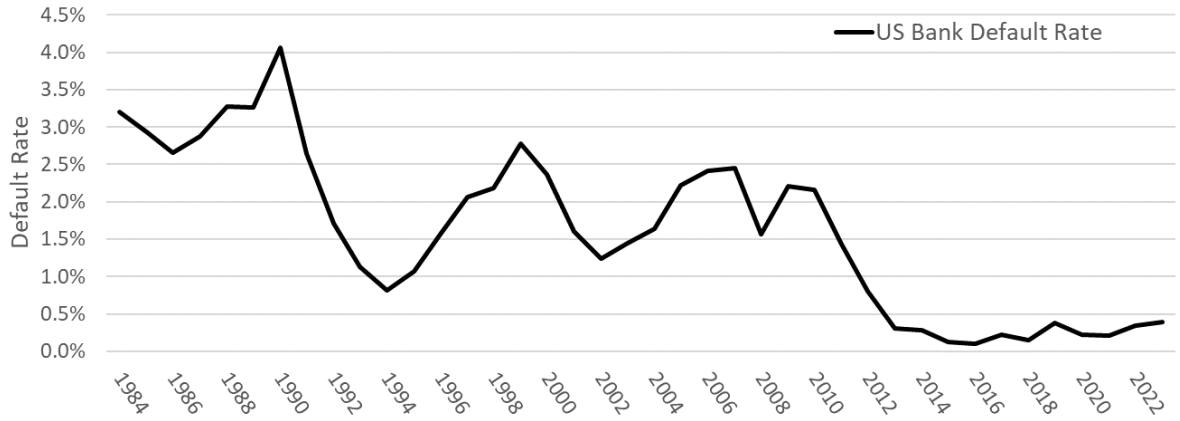


Source: Federal Deposit Insurance Corporation (FDIC), commercial banks only.